EFFECTS OF EXTRUSION COOKING OF CORN AND MILO ON ALCOHOL PRODUCTION

By

JOHN MUNGER O'NEAL

Bachelor of Science

in Agricultural Engineering

Oklahoma State University

Stillwater, Oklahoma

1980

Submitted to the Faculty of the
Graduate College of the
Oklahoma State University
in partial fulfillment of
the requirements for
the Degree of
MASTER OF SCIENCE
May, 1983

EFFECTS OF EXTRUSION COOKING OF CORN
AND MILO ON ALCOHOL PRODUCTION

Thesis Approved:

Bobby L. Clary
Thesis Adviser

A. D. Barefoot

James E. Garton

Norman N. Durham
Dean of Graduate College

PREFACE

The research reported in this thesis was financed in part by the Oklahoma Wheat Commission.

The author expresses sincere appreciation to Dr. Bobby L. Clary for his excellent professional and personal guidance during the course of this study. Dr. Clary was always willing to offer assistance and his continuous encouragement was invaluable. Dr. Clary was also responsible primarily for the author having pursued a M.S. degree at Oklahoma State University.

He also wishes to express his gratitude to Professor Willard Downs for his ready availability and willingness to offer advice. Professor Downs was always willing to confer with the author on professional or personal problems. Special appreciation is extended to Professor Downs.

The advice and counseling of the other members of the committee, Dr. James E. Garton and Professor A. D. Barefoot, was very much appreciated.

The author is grateful to Jack Fryrear for his excellent preparation of the illustrative material. The assistance and advice of Mr. Norvil Cole was also deeply appreciated.

I thank the Agricultural Engineering Department, headed by Dr. C. T. Haan, for creating a desirable atmosphere within which to study and work and for providing the assistantship which made this thesis possible.

Finally, I thank my wife, Rickie Louise, and my children, Robert and Melissa, for their encouragement, love, and extreme patience and my parents for their love, support, and encouragement.

TABLE OF CONTENTS

LIST OF TABLES

Table		Page

LIST OF FIGURES

Figure		Page

Figure		Page

LIST OF SYMBOLS

N	=	sample number
DA	=	test date
GT	=	grain type (ground corn or milo)
STE	=	steam lock configuration
MC_i	=	initial moisture content of the grain (wet basis)
MC_f	=	final moisture content after extrusion (wet basis)
MC_e	=	extrusion moisture content (wet basis)
ΔP	=	difference in pressure across the orifice on the water metering system (PSI)
$\dot{m}_w$	=	lbm/hr of water added due ΔP
T_1	=	average exit temperature (°F)
T_2	=	average transition zone temperature (°F)
T_3	=	average entrance section temperature (°F)
$\dot{m}_p$	=	product flow rate (dry basis)
G_e	=	glucose value of extruded grain (mg/dl)
S_e	=	starch conversion in the extruded sample (%)
G_b	=	glucose value of batch cooked sample (mg/dl)
S_b	=	starch conversion in the batch cooked sample (%)

G_i = glucose value of the background sample (mg/dl)

S_i = total starch in background sample (%)

R_1 = temperature gradient for the forward section of the extruder barrel

R_2 = temperature gradient for the rear section of the extruder barrel

T_f = fractional part of the total temperature change in the front end of the extruder barrel

CHAPTER I

INTRODUCTION

The Problem

With the increased demand on all energy sources, the efficiency of systems which transform energy into a more usable form are receiving much attention. As in the case of the production of ethanol for fuel, there has been a great deal of interest in obtaining higher yields per bushel of grain. Many small fuel alcohol plants have been installed across the United States. Most of these facilities are at the farmstead level, but there are also those which can be considered of commercial size. Most of these facilities have borrowed the technology used in the beverage alcohol industry and adapted it for fuel alcohol production. The need for new process equipment and new technologies for the fuel alcohol industry is a must if alcohol is to become a viable, economic source of liquid fuel.

The typical fuel alcohol plant uses what is known as the batch system. In this type of system, one large quantity of grain and water is cooked and then saccharified. The distillation system can be continuous if the initial "batches" are of sufficient size to accommodate the process. One of the major consumers of energy in the batch type system is the cooking process. This process involves the addition of water and grain, in predetermined quantities, into a large tank. Large quantities of heat must be added in this stage. Heat transfer characteristics in the typical cook tank are poor, requiring high thermal capacities which causes the total energy input to increase. Heat loss due to thermal conductivity of the walls of the cook tank combined with the loss to the atmosphere also contribute to higher energy input.

Another serious problem with the batch cook system is conversion of starches to dextrins to alcohol. These methods require strict temperature and pH control. Systems that do not have control over these parameters can cause a negative energy balance, making the fuel alcohol process an uneconomic venture. Batch cooking requires that variables such as temperature and pH be maintained at specific requirements. The inertia denoted by the size of the process equipment can cause problems in controlling temperatures and pH during cooking and saccharification. The cooking process in the batch system may not be providing adequate temperatures or holding times. The process must break the cell walls of the starch, allowing the complex sugars produced to be further reduced to dextrose.

In the extruder, cooking characteristics similar to the batch system are encountered, but the grain is cooked at a much higher temperature and a high shear rate is introduced. The extruder also has a low residence time compared to batch cooking. This may provide more cell wall rupture which leads to availability of more dextrins per unit of enzyme. Gelatinization (cell wall rupture) combined with high temperatures may also provide for the discontinuance of the use of a liquefying enzyme (alpha-amylase). The extruder can become an important part of the cooking process due to this gelatinization effect. Even at long holding times of 2.5 to 3.0 hours in a batch system, all the starch molecules will not be converted to soluble dextrins. The extruder can cause an increased conversion of starch to soluble dextrins.

The development of more efficient cooking techniques is definitely a need if the fuel alcohol process is to be economic.

Objectives

The specific objectives of this research are:

1. to determine the effect of temperature, moisture content, and product flow rate on conversion of starch to dextrose when using an extrusion cooked grain product.

2. to compare the starch to ethanol conversion observed when using an extruded grain product to the conversion observed when using a conventional batch cooked process.

3. to determine the optimum extrusion temperatures and extrusion moisture content for corn and milo.

CHAPTER II

REVIEW OF LITERATURE

The Batch System

The most commonly used process for fuel alcohol production is the batch system. There are basically two main divisions which can be made. The first is the conversion of starches to simple sugars and sugars to alcohol while the second is the distillation of the water-alcohol mixture. There are several distillation techniques available, some with minor alterations such as heat recovery, which are considered to be the state of the art. Most of these processes have been accepted to be sufficiently efficient to operate in conjunction with fuel alcohol plants.

The basic chemical equation for conversion of starch materials to alcohol is:

$$\underset{\text{(starch)}}{C_6H_{10}O_5} + H_2O \xrightarrow{\text{addition of enzymes}} \underset{\text{(glucose)}}{C_6H_{12}O_6} \xrightarrow{\text{addition of yeast}} \underset{\text{(ethanol)}}{2C_2H_5OH} + \underset{\text{(carbon dioxide)}}{2CO_2} + \text{heat}$$

Figure 1 illustrates the basic flow diagram of a plant using cereal grains as the feedstock. Grain must be brought to the plant so there must be adequate storage depending on

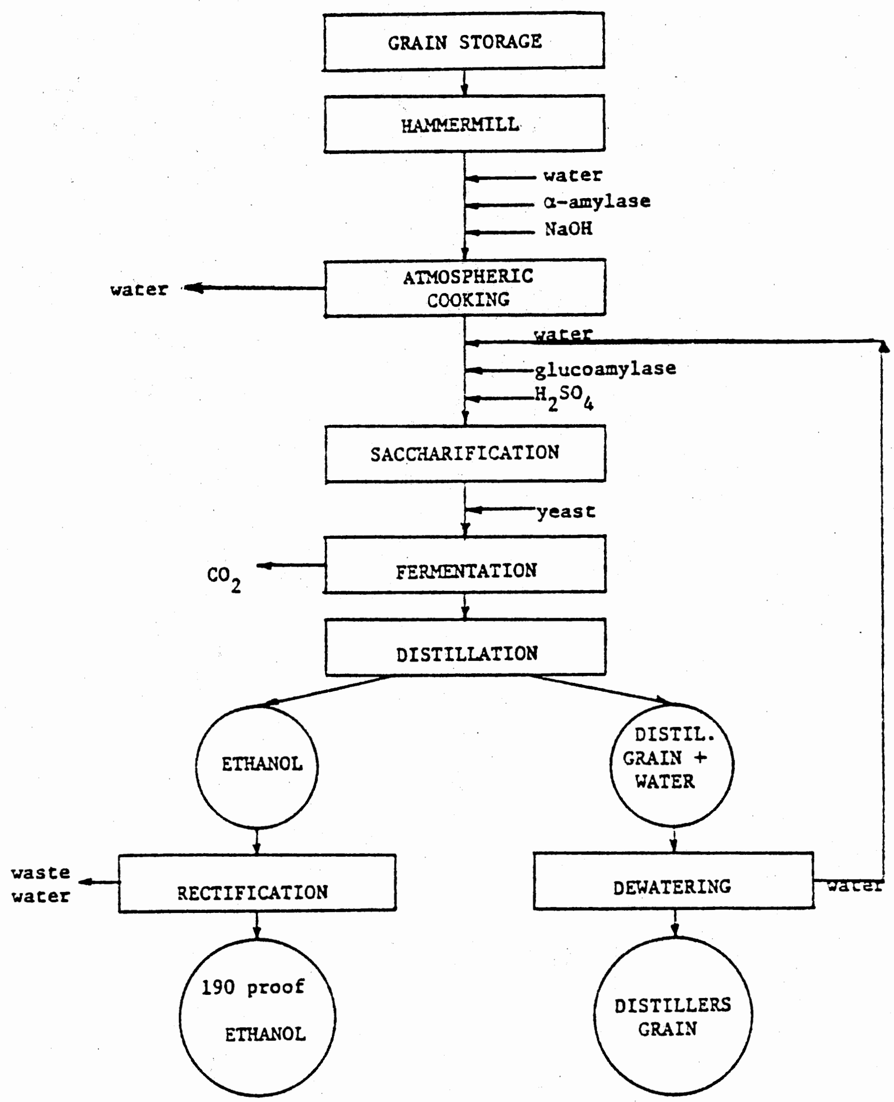

Figure 1. Processing block diagram for conventional processing of grain to ethanol production.

the size of the plant. From storage, grain is processed through a hammermill to produce an average particle size of 40 mesh. At this time, approximately 15 gallons of water per bushel of grain is added and the slurry is cooked at 205°F for approximately one hour to solubilize the starches. The pH is adjusted to between 6.0 and 7.0 by the addition of sodium hydroxide. During cooking the addition of an alpha-amylase enzyme will help break down the long polysaccharide chain into smaller chains of glucose called dextrins and reduce slurry viscosity. After cooking, the slurry is cooled to 140°F to 160°F by addition of water. In some systems, a second dose of an alpha-amylase is added at this time to provide for continued breakdown of the alpha-(1-4) bonds. The slurry is then cooled to 80-90°F by adding water which will bring the total volume of water to approximately 30 gallons per bushel. The pH is adjusted to a range within 4.0 to 4.5 by the addition of sulfuric acid. At this time the addition of an amyloglucosidase enzyme is used to randomly break the alpha-(1-4) starch molecule bonds by splitting off single residues of glucose from dextrins, producing single (glucose) sugars. At this same stage in the process, the slurry is inoculated with a yeast culture (saccharomyces) and allowed to ferment from 48 to 60 hours at 85 to 90°F. Fermentation is the process in which simple sugars are converted to ethanol. Heat is one product of the chemical reaction of fermentation,

$$C_6H_{10}O_6 \dashrightarrow 2C_2H_5OH + 2CO_2 + \text{heat},$$

therefore, cooling during fermentation is essential since most yeast cultures are destroyed at temperatures exceeding 105°F. Excessive temperatures result in a significant reduction of alcohol yield per bushel. A typical fuel alcohol plant will use a "menu" similar to the one given in Appendix A.

Extruders

Extrusion is a well known process in the food industry. It originated in the plastics industry, where its first use was for forming plastic pipe (ex. PVC pipe). Some applications of the extruder in the food industry are breakfast cereals, pet foods, snacks, and various blended foods.

There are basically two types of single screw extruders; hot (dry extrusion) and cold (high moisture extrusion). The initial moisture content for material extruded in dry extruders ranges from 10 to 20 percent while wet extrusion involves material with moisture content of 25 percent or higher. Cold extruders are designed to extrude a material without the generation of heat, without cooking and without any distortion of the product as it exits from the extruder. For this reason cold extruders are used for sizing a product and usually have slow turning shafts designed for low shear. Hot extruders are designed to generate heat by shear and friction developed by a rapidly rotating shaft working against the material to be extruded. They are used to cook raw input materials and are designed to permit accurate sizing as well as puffing of a product.

There are several advantages of grain extrusion that are of particular interest. A wide variety of ingredients can be used on the same basic extruder with similar processing conditions. An extruder provides a continuous processing system having greater production capability than other cooking systems. Another very desirable advantage is high product quality. The short, high-temperature treatment destroys most undesirable factors in food. Some examples of these factors are trypsin inhibitors, undesirable enzymes, and microorganisms.

A food extruder consists of a flighted Archimedes Screw which rotates in a tightly fitting cylindrical barrel. The feed material is usually preground and may be blended with a variety of ingredients before extrusion. Preconditioning of the material to be extruded consists of preheating and/or varying the moisture content. Heat is added to the food dough as it passes through the screw by one or more of three mechanisms: (1) viscous dissipation of mechanical energy being added to the shaft of the screw, (2) heat transfer from steam or electrical heaters surrounding the barrel, and (3) direct injection of steam which is mixed with the dough in the screw (Harper, 1981). As the grain and the ingredients added move down the barrel, the pressure increases due to the restriction at the discharge end of the barrel. At this high pressure, boiling and flashing do not occur inside the barrel due to the pressure in the barrel exceeding the vapor pressure of water at the extrusion temperature. As the extruded material emerges from the discharge end of the barrel, this pressure is lost causing the rapid expansion of the exiting material with excessive flashing of moisture. The loss of moisture due to flashing causes the product to solidify and retain the approximate shape as when it expanded. This causes the product to appear very light and fluffy. As the product is transported through the barrel, high shear rates are encountered due to the area between the screw and the barrel being full. This high shear rate is one reason for the high temperatures encountered and also causes a restructuring of the molecular configuration of the grain.

The extruder can be broken into four main components: the feed mechanism, the rotor, the thrust bearing and the barrel (Figure 2). To better understand the effect of extrusion processing of foods, a discussion of these components is needed.

The thrust bearing is required to support and center the extrusion screw and absorb the thrust exerted by the screw. Since the screw forces food forward against a back pressure, a rearward thrust is produced on the screw which must be absorbed by the thrust bearing. The magnitude of the thrust is approximated by the maximum extrusion pressure times the cross-sectional area of the barrel.

The feed mechanism is a device for providing a uniform

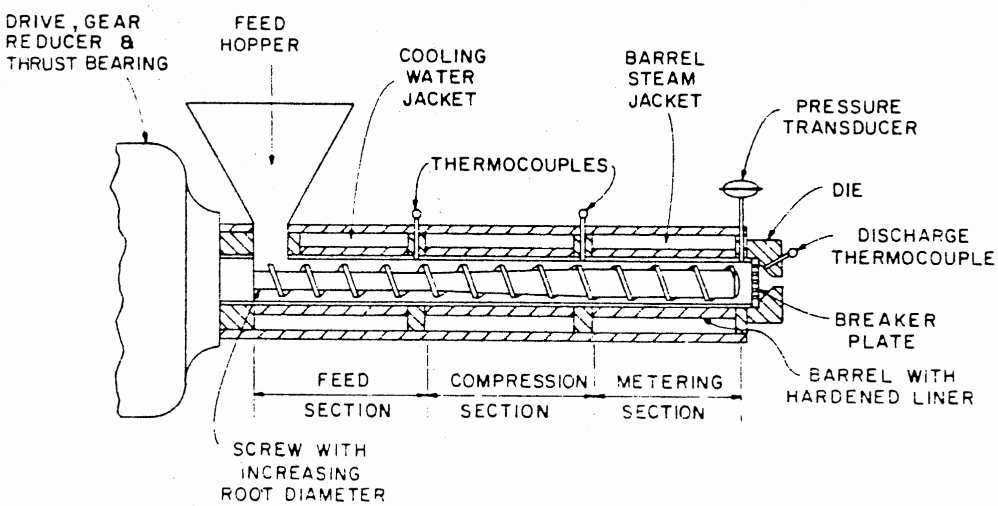

Source: Harper (1981)

Figure 2. Cross-section of a typical food extruder.

delivery of food ingredients which are often sticky, non-free-flowing substances. A number of feeding devices are used including the following. Vibratory feeders consist of a vibrating pan which has either variable frequency or stroke and is used to control the feed rate from a hopper. Variable speed augers are screw conveyors having a variable speed auger which can be used to volumetrically meter relatively free-flowing food ingredients. Weigh belts are also used in extruder processes. A weigh belt is a moving belt with a weighing device under the central section of the belt and is used to gravimetrically meter food ingredients. Two types of weigh belts exist; one with a variable feed gate opening to the belt and the other having a variable speed belt with a fixed gate. Signals from the weighing device adjust either the gate opening or belt speed to accomplish a uniform feed rate.

The screw is the central portion of a food extruder. It accepts the feed ingredients at the feed port, conveys, works, and forces them through the die restriction at the discharge. The extrusion screw is divided into three sections (as shown in Figure 2) whose names correspond to the function each section plays. The feed section is the portion of the screw which accepts the food materials. The feed section can usually be characterized by deep flights, indicating the function of assuring sufficient material is conveyed down the screw and the screw is completely filled. The compression section is sometimes called the transition zone. The ingredients are normally heated and worked into a continuous dough mass during passage through the transition zone. The transition zone is commonly the longest section of the screw, taking approximately half of its length. There are several ways to achieve compression in an extruder. These are outlined in Figure 3, showing several different screw-barrel configurations. The metering section is characterized by very shallow flights. The shallow flights increase the shear rate in the channel to the maximum level within the screw. The viscous dissipation of mechanical energy is typically large in the metering section so that the temperature increases rapidly. The extruder barrel is the cylindrical member which fits tightly around the rotating extruder screw. When heating the product by outside sources is required, a variety of heating elements can be placed directly around the barrel to accomplish this task.

Starch

The Structure of Starch

Starch constitutes the major food reserve material of all the higher plants. It is inside small cells (plastids) in the form of particles that are insoluble in cold water. Starch granules are comprised of multiple plastids. Starch can be defined as a carbohydrate, more particularly a high-molecular weight polysaccharide, having the empirical formula

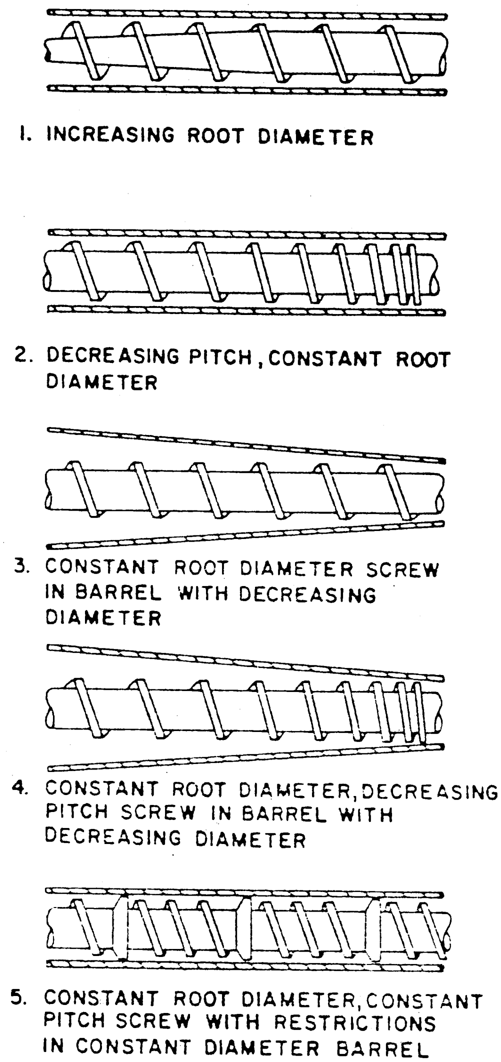

Source: Harper (1979)

Figure 3. Varying configuration of screw and barrel to achieve compression.

$$(C_6H_{10}O_5)n$$

where the value of n is large but not accurately known. Polysaccharides are polymers of sugar, and their hydroxyl groups enable them to form pastes with water. Starch itself is considered to be made up of two molecular constituents: amylase a straight chain and amylopectin, a branched structure. Their proportion and the number of repeating groups per starch molecule is presumed to vary widely between starches of different origin. Also, the precise way in which amylase and amylopectin are associated in the granule is not known (Manners, 1968). The major component, amylopectin, amounts to 75 - 85 percent of most starches, and has a branched structure in which chains containing on the average of about 20-25 alpha-(1-4) linked glucose residues are interlinked by alpha-(1-6) glucosidic linkages. Manners (1968) depicts amylopectin as a bush like structure (Figure 4). Amylase, the minor component, is an essentially linear polymer of glucose containing more than 99 percent of alpha-(1-4) glucosidic linkages. The amylose content of most starches is 15 - 25 percent.

Figure 5 depicts a molecule of starch, which is made up of the monosaccharide glucose. There are two different types of bonds in starch molecules; the alpha-(1-4) and the alpha-(1-6). The alpha-(1-6) bonds are found on the branching segments, amylopectin, and the alpha-(1-4) bonds are found in the straight chains, amylose. Enzymes are

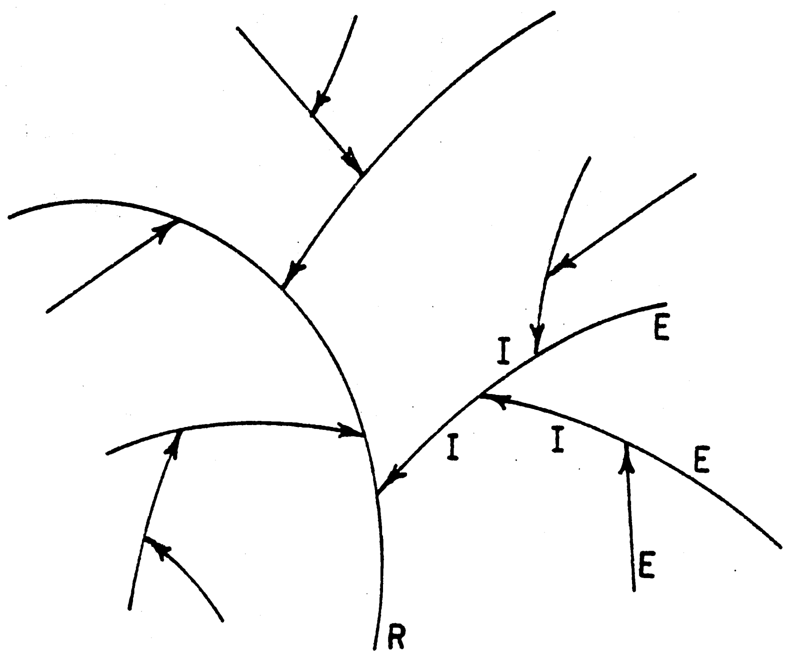

Key: — linear chain of alpha-(1-4) linked glucose residues
← alpha-(1-6) inter-chain linkage
I interior chain
E exterior chain
R reducing group

Figure 4. Multiple-branched structure for amylopectin (redrawn from Radley (1968)).

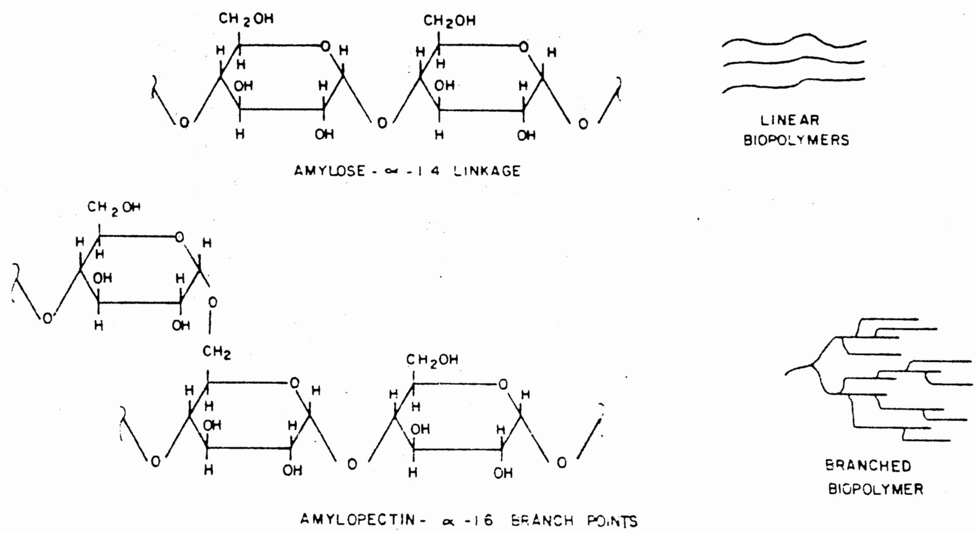

Source: Harper (1981)

Figure 5. Structure of amylose and amylopectin.

available which will break these bonds, forming single molecules of glucose.

Properties of the Starch Granule

The generally accepted starch model depicts the starch granule as spherocrystalline being built up on concentric layers or growth rings. In each layer, the intermingled molecules are laid down in radial fashion during growth around a central region called the hilum. This structure is believed to be responsible for the birefringence of the starch granule when viewed under polarized light.

The volume of starch that is in contact with water is variable. This is due to the ability of starch to absorb water (some up to 40 percent of their original weight) which causes a volumetric expansion. The higher the temperature, the less water is absorbed, although at the temperature where swelling begins this is no longer true.

All properties of the starch granule are related to a combination of two factors, namely: its chemical constitution, depending on the presence of the two major discrete components, amylose and amylopectin; and its physical constitution, involving the organization of these polymers to form a unique structural entity. The granules themselves vary considerably in shape and size, so much so that the source of a starch can be identified merely from its microscopic appearance. To characterize the starch granule it is necessary to determine the arrangement of molecules within the granule. Banks and Greenwood (1975) indicate it has been accepted that starch is a semi-crystalline material. The basic structural type of most starches of cereal origin are similar, as compared to starches of potatoes, peas, beans, etc.

Swelling and Gelatinization of Starch

Kerr (1950) states that in its natural state, starch is insoluble in cold water but appears to absorb about 25 to 30 percent and does not swell appreciably. With rising temperature, the hydrogen bonds that hold the structural units together and the solvent water molecules in an aggregated state tend to dissociate. The smaller dissociated water molecules, when at a higher energy level, are able to permeate the weakened starch structure and gradually hydrate the many hydroxyl groups along the length of the starch molecules. According to Kerr (1950), at 60°C, corn starch takes up about 300 percent water and at 70°C, about 1000 percent, based on its original weight. At the point of maximum swelling the granule can take up 2500 percent, so that not more than 4 percent of dry substance is present.

The temperature at which there is an apparent change in the appearance of the granule is called the swelling temperature. The unswollen starch granule shows a cross when viewed under polarized light, and this effect is lost when swelling occurs. Apart from swelling, a number of other changes occur. The granules begin to lose their birefringence, the solubility of starch increases due to the loss of low-molecular-weight amylose from the granules, and the solution becomes viscous and sticky. If the solution of gelatinized starch is sufficiently concentrated it will set to a rigid gel on cooling to room temperature.

Since starch swelling is dependent on the nature of the granule structure, it is not surprising that mechanical injury to the granules causes increased swelling. Kerr (1950) noted that over-grinding of flour resulted in the appearance of injured starch granules. These undergo marked swelling, even in cold water. Therefore, it is very likely that the extruder would affect the grain in the same manner.

Harper (1981) describes the gelatinization process diagrammatically as shown in Figure 6. Initially, the water added will disrupt the ordered structure. As the process continues, the starch granules swell and may increase their volume by 30-fold. As more heat and water are added, the amylose begins to diffuse out of the granules and the starch is no longer in the reversible state (cannot return to it's original form). As the gelatinization process continues, the granules collapse and more and more water molecules attach themselves to the exposed hydroxyl groups on the starch chain. A gel structure results with the amylose supporting the collapsed granules consisting mostly of amylopectin.

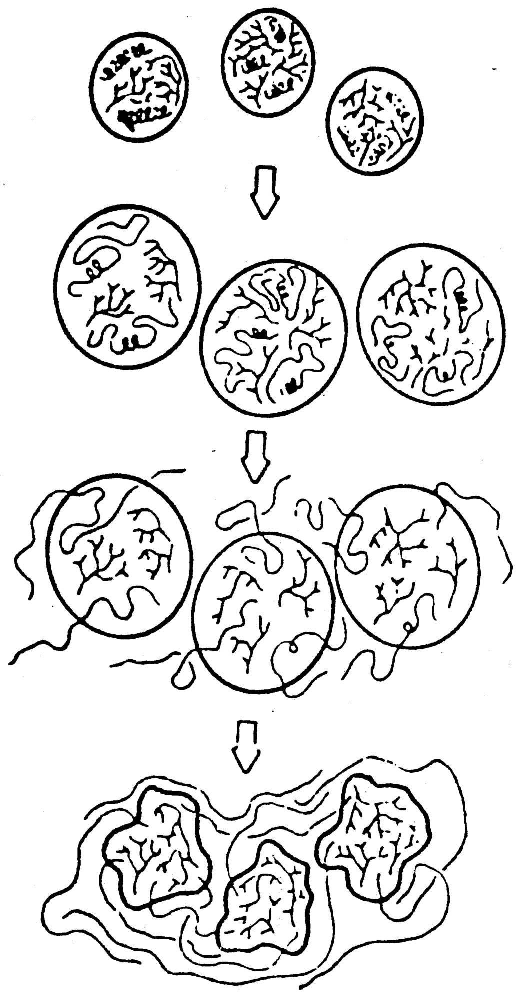

Raw starch granules made up of amylose (helix) and amylopectin (branched).

Addition of water breaks up amylose crystallinity and disrupts helices. Granules swell.

Addition of heat and more water causes more swelling. Amylose begins to diffuse out of granule.

Granules, now containing mostly amylopectin, have collapsed and are held in a matrix of amylose forming a gel.

Figure 6. Mechanism for starch gelatinization (redrawn from Harper (1981).

Extrusion of Starches and Starchy Materials

Extensive literature exists on the gelatinization of dilute mixtures of starch with water. In contrast, very little information is available on the gelatinization of starch at moistures less than 50 percent, the range where extrusion processing is practiced.

Results obtained by Mercier (1975) show several effects of extrusion. Cereal starches (22 percent moisture content) were extruded at different temperatures between 70 and 225°C. Waxy corn, corn, common wheat, rice, Amylon-5, and Amylon-7 starches were compared. Changes in final cooked-paste viscosity (50°C), water absorption index, and water-solubility index of extruded products as related to increasing extrusion temperature are given in Figures 7 and 8. Susceptibility to alpha-amylase increases with increasing extrusion temperature but was different depending on whether determinations were made on the whole extruded product or after milling.

For an extrusion temperature of 135°C, the initial rate of alpha-amylolysis of the milled extruded products (Figure 7, Vi-milled) was similar for waxy corn, normal corn, wheat, and rice, corresponding to 20 percent of starch being degraded in the first five minutes. Vi was lower for Amylon-5 and Amylon-7. The same phenomenon was observed for the easily degradable fraction of starch, F (Figure 7, F-milled).

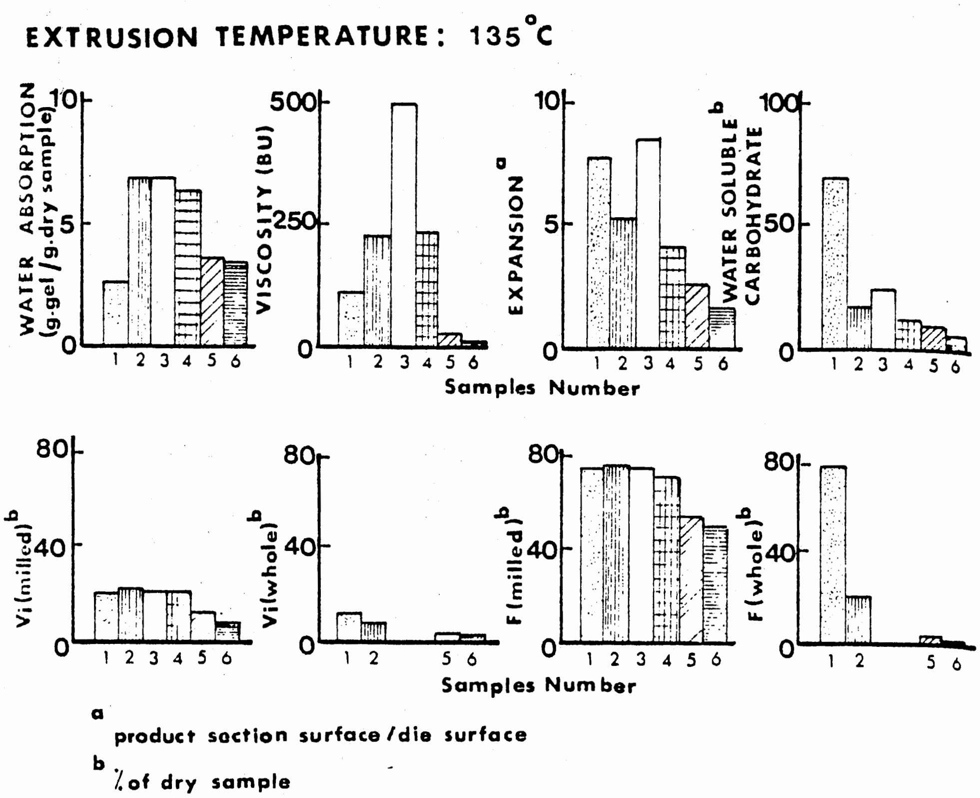

Source: Mercier (1975)

Figure 7. Water absorption index, viscosity (50°C), expansion, water-soluble carbohydrate, Vi, and F (alpha-amylolsis parameters) on products extruded at 135°C. Starches: 1) waxy corn; 2) corn; 3) common wheat; 4) rice 5) Amylon 5; 6) Amylon 7. Initial moisture content before extrusion was 22% by weight.

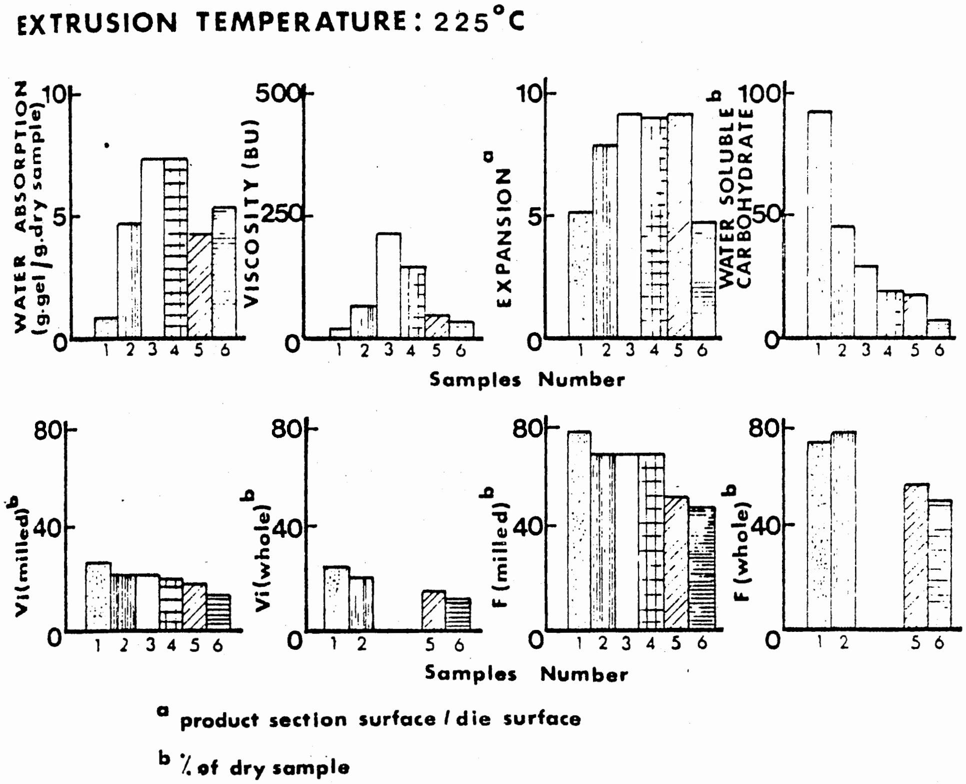

Source: Mercier (1975)

Figure 8. Water absorption index, viscosity (50°C), expansion, water-soluble carbohydrate, Vi, and F (alpha-amylolsis parameters) on products extruded at 225°C. Starches: 1) waxy corn; 2) corn; 3) common wheat; 4) rice; 5) Amylon 5; 6) Amylon 7. Initial moisture content before extrusion was 22% by weight.

For whole extruded products, the results were different. The initial rate, Vi, was reduced to half (10 percent of waxy corn starch degraded in the first five minutes) that of milled products. Furthermore, a significant difference has been observed between starches. Whereas whole or milled extruded waxy corn did not show any difference for F, this last parameter decreased significantly from normal corn to Amylon-5 and Amylon-7. At this low extrusion temperature, expansion was reduced. Therefore, it is likely that attack by alpha-amylase, which depends on penetration of the enzyme into the substrate, is much faster and easier on the milled extruded product than on the whole extruded one. This is caused because the surface available to the enzyme is much greater.

No significant difference was observed in Merciers (1975) work when the parameters Vi and F (Figure 8) were determined for both whole and milled extruded products at an extrusion temperature of 225° C. At this extrusion temperature, the extruded products were expanded in such a way that the enzymes easily penetrated the product.

Chiang (1977) reported on some important factors affecting starch gelatinization during extrusion of wheat flour, such as moisture content of raw materials, temperature, screw speed, and die nozzle size. Figure 9 shows the results relating the effect of moisture and temperature on wheat starch gelatinization. Temperatures of about 80°C sharply increase the gelatinization of the starch in the

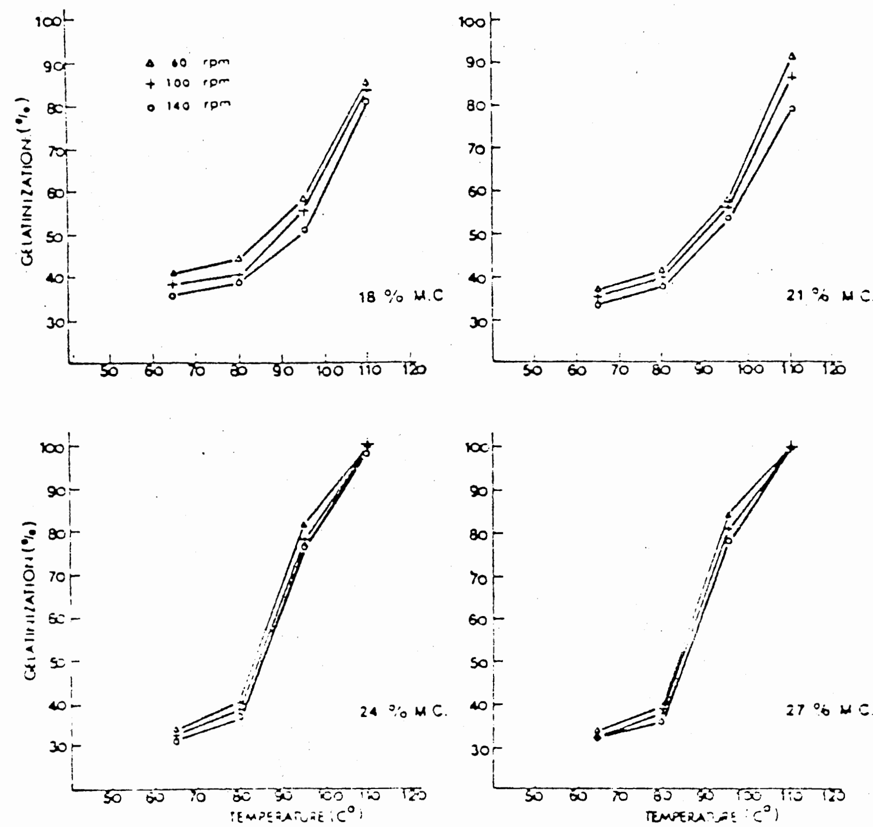

Source: Chiang (1977)

Figure 9. The effect of temperature, screw speed, and moisture on wheat flour gelatinization.

sample. Moisture content over the range studied had a lesser effect on gelatinization, but higher moisture contents gave greater percentages of gelatinization. The effect of screw speed is also shown in Figure 9. As screw speed increased, the percent gelatinization decreased. This is due to the shorter residence times associated with higher screw speeds.

The effect of die size is shown in Figure 10. Chiang (1977) reports that as the die nozzle size increases, the percent gelatinization decreases. This is caused by the effect of decreasing back pressure and decreasing shear rate as the die size increases.

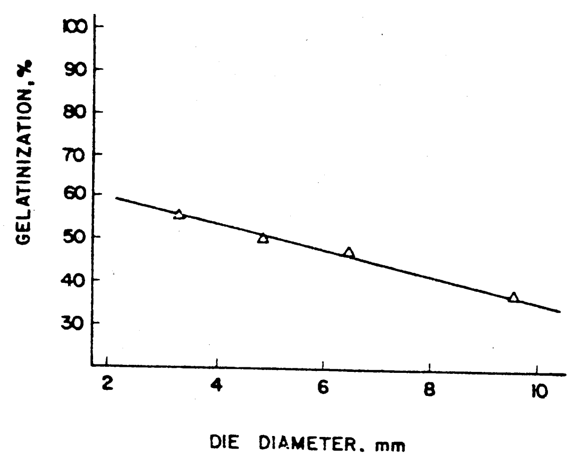

Source: Chiang (1977)

Figure 10. Effect of die diameter on wheat flour gelatinization.

CHAPTER III

MATERIAL AND EXPERIMENTAL EQUIPMENT

The Insta-Pro 500

The Insta-Pro 500 used in this study has two feed mechanisms (Figure 11). The vibratory feed system is used for initial start-up of the extruder. Material used for this process is commonly soybeans because of the need for a high oil content. The volumetric feeder is simply a screw feeder in which a constant rate of material can be directly injected in the side of the barrel. This feeder contains the material that is to be extruded.

The Insta-Pro 500 is designed to transform mechanical energy from its fifty horsepower electric motor into thermal and shear energy. This is accomplished with the screw and rotor. The mechanical energy input into the rotor causes high friction and shear rates in the barrel, which results in the development of high temperatures and pressures. These conditions provide starch gelatinization and the restructure of carbohydrate components.

The rotor and barrel (Figure 11) of the Insta-Pro 500 can be described by separating it into three functions. The first section is the feed section where the material is

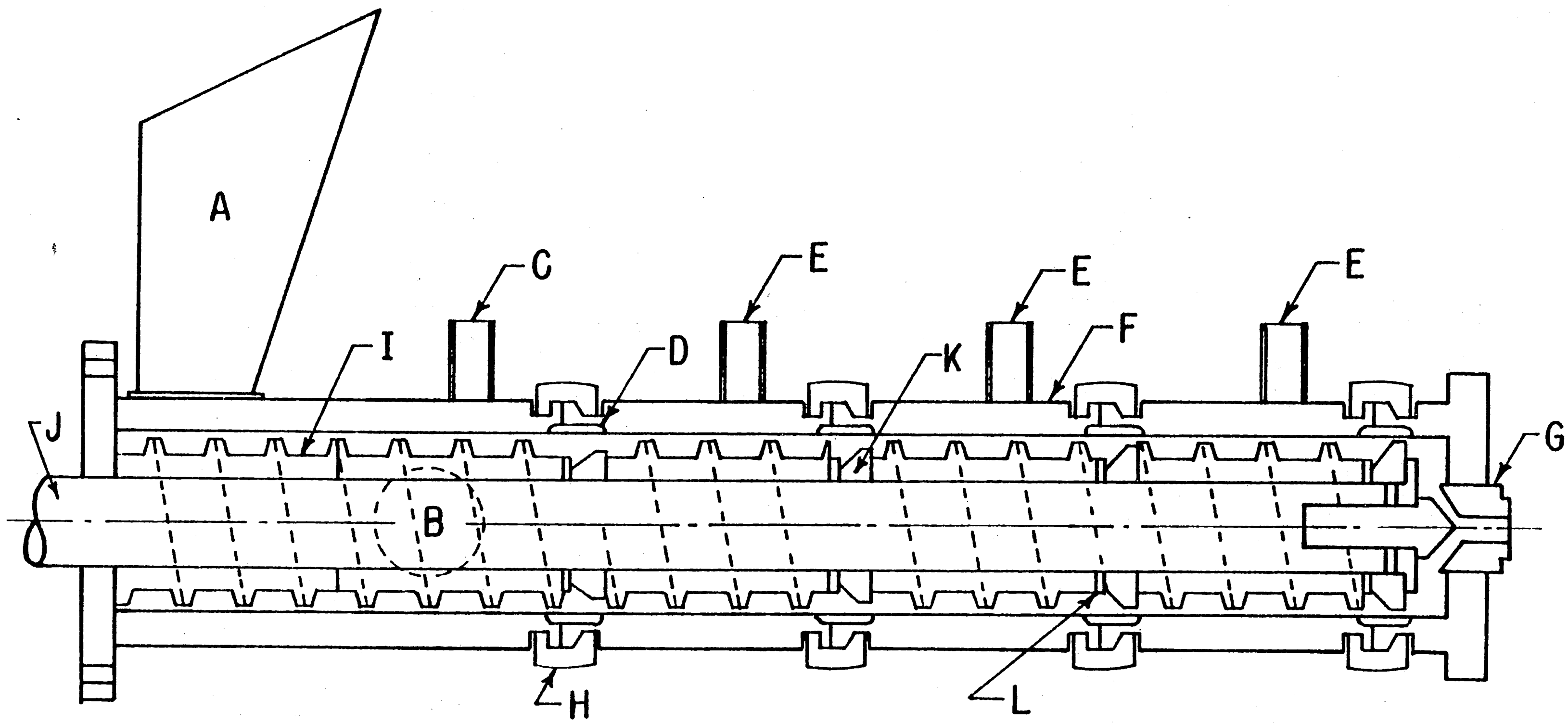

A.	Vibratory Feeder Entrance Section	G.	Orifice
B.	Volumetric Feeder Entrance Section	H.	Barrel Segment Clamps
C.	Water Injection Port	I.	Screw Sections
D.	Wear Rings	J.	Shaft
E.	Thermocouple Ports	K.	Steam Locks
F.	Barrel Segments	L.	Spacers

Figure 11. The Insta-Pro 500 Extruder Configuration.

fed into the barrel by the screw. The second section is the transition zone. In this section, shear forces become greater and structure of the material being extruded begins to change. The temperature also starts to increase in this section, causing the material to form into dough. The third section is the metering section, where even higher temperatures are encountered as shear rates increase. The material in this section is then forced to flow through an orifice. Upon contact with atmospheric temperature and pressure, the product is transformed by exothermic expansion, causing super-heated water vapor to flash off. This flashing causes the product to expand rapidly, forming a "puffed" effect.

The Insta-Pro 500 is equipped with removable screws and steam locks. The screws can be replaced by "single flighted" or "double flighted" screws (Figure 12). There are also four sizes of steam locks available (Figure 13). With these two variables, there are numerous configurations available for operation at different temperatures and pressures. The moisture content may be varied, thereby producing different sample characteristics for one particular screw configuration.

Figure 14 shows geometry of the Insta-Pro screw and barrel section. Internal diameter of the barrel in which the screw rotates is denoted as D. The actual screw diameter accounting for the clearance, δ, is D_s.

The dimension between the barrel surface and root of

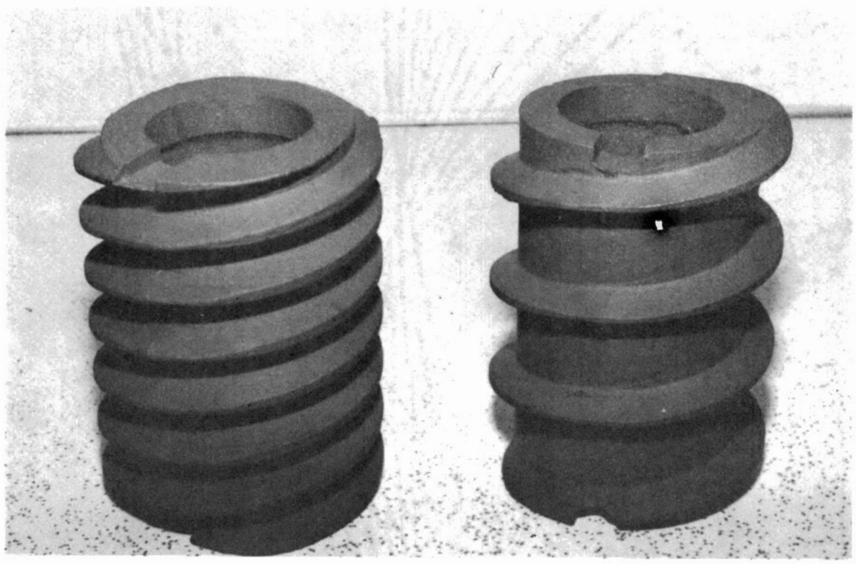

Figure 12. Two types of screw sections available for the Insta-Pro 500.

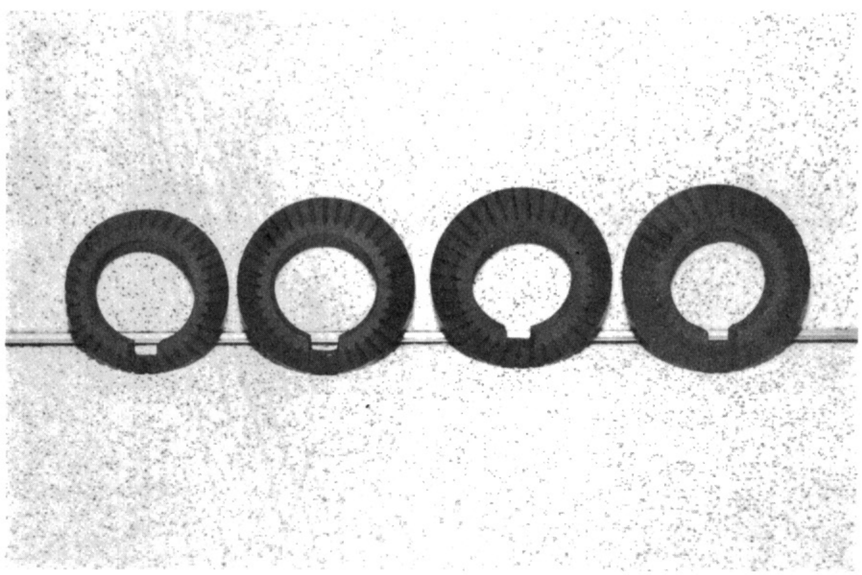

Figure 13. Four sizes of steam locks available for the Insta-Pro 500.

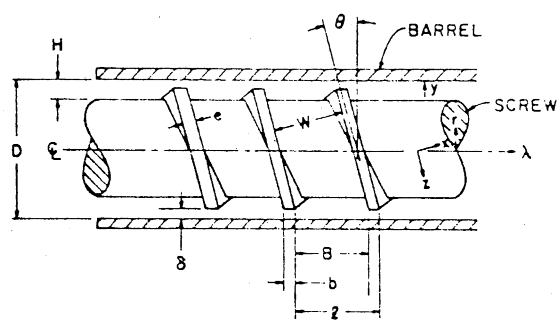

Figure 14. Geometry of the Insta-Pro 500 screw and barrel section.

the screw is defined as H. The actual flight height of the screw is H_s. The root diameter, D_r, is the diameter of the root of the screw. The diametral screw clearance, is the difference between the diameter of the screw and bore of the barrel. Lead, ℓ, is the axial distance from the leading edge of a flight at it's outside diameter to the leading edge of the same flight in front of it. The helix angle, Θ, defines the angle which the flight makes with a plane normal to the axis of the screw. Axial channel width, B, is the axial distance from the leading edge of one flight to the trailing edge of the same flight one complete turn away at the diameter of the screw. The channel width, W, is the channel width measured as above but perpendicular to the flight. The axial flight width, b, is the axial width of a flight measured at the diameter of the screw. Flight width, e, is the flight width measured perpendicular to the face of the flight. The particular values for the Insta-Pro 500 set up with single flighted screws are as follows:

δ = 0.10 inch

D_s = 3.67 inch

H_s = 0.34 inch

D_r = 2.99 inch

ℓ = 1.37 inch

Θ = 6.8 deg.

B = 1.25 inch

b = 0.125 inch

e = 0.124 inch

The YSI Model 27

The YSI (Yellow Springs Instrument) Model 27 Industrial Analyzer (Figure 15) is intended for quantitative determination of the concentration of dextrose (glucose), sucrose, and lactose in foodstuffs of other nonclinical materials (YSI 27 Instruction Manual,1975). It offers precision comparable to more time consuming and rigorous methods, but with greater speed and convenience. Measurements are virtually unaffected by sample color, turbidity, density, viscosity, pH, volatility, specific gravity, temperature, index of refraction, optical activity, or presence of other nutrients.

Samples to be analyzed in the YSI Model 27 must be fluids. Solid specimens must be dissolved, extracted, liquified or slurried prior to analysis. Merely allowing a solid material to stand in contact with a measured volume of water may be sufficient. Reducing agents of very low molecular weight, such as hydrazine, hydrogen sulfide and certain thiols interfere with the operation of the Model 27 and must not be present. High levels of some phenols and anilines will also cause erroneously high readings. To determine if any of these materials are present, non-enzymatic "blank" membranes can be used with the YSI 27. Concentrated acids or bases must be approximately neutralized to the range of pH 5 to pH 8 before injection. For greatest precision, samples should be near the temperature of the calibration solution. A 25 microliter specimen

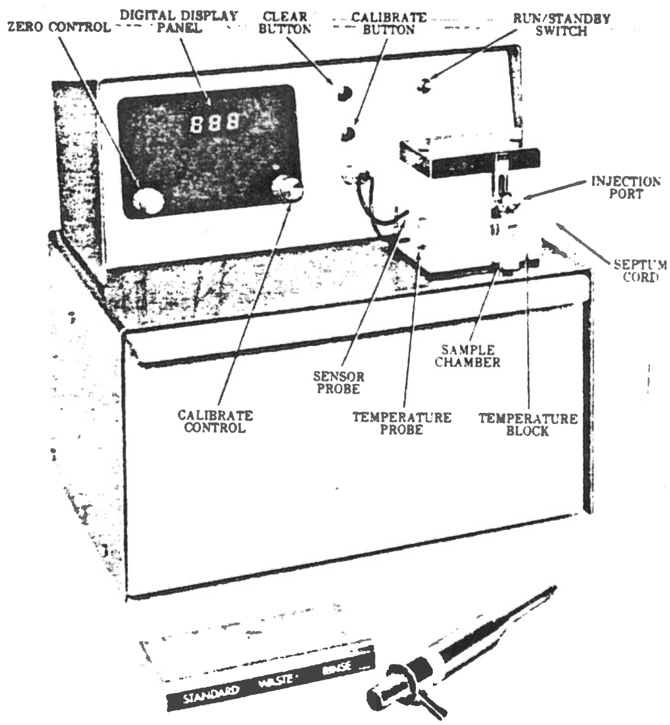

Figure 15. The YSI Industrial Analyzer.

volume is required for the operation of the YSI 27, permitting small sample volumes.

The sensor probe (Figures 15 and 16) of the YSI 27 contains an electrode system which responds to hydrogen peroxide. Current flow in the platinum anode circuit is linearly proportional to the local concentration of hydrogen peroxide. The circuit is completed by a silver cathode. At constant chloride concentration, the potential of this reaction is practically independent of current, so the silver electrode provides a stable reference potential.

The membrane which fits over the sensor face is a three-layer laminate, with the middle layer containing one or more immobilized enzymes. These enzymes convert the substance to be measured into hydrogen peroxide; the hydrogen peroxide is measured by the platinum anode and the result is a signal current proportional to the concentration of the substance to be measured. The YSI 27 converts this signal current to a voltage, scales the signal according to the ZERO and CALIBRATE controls, and displays the assay value on a digital meter.

The middle layer of the dextrose membrane contains the immobilized enzyme glucose oxidase. Glucose oxidase catalyzes a reaction to yield hydrogen peroxide.

Figure 16 shows an exploded view of the membrane and its relationship to the sensor face. Glucose, which has been diluted by the buffer in the sample chamber, first diffuses through the polycarbonate membrane. This membrane

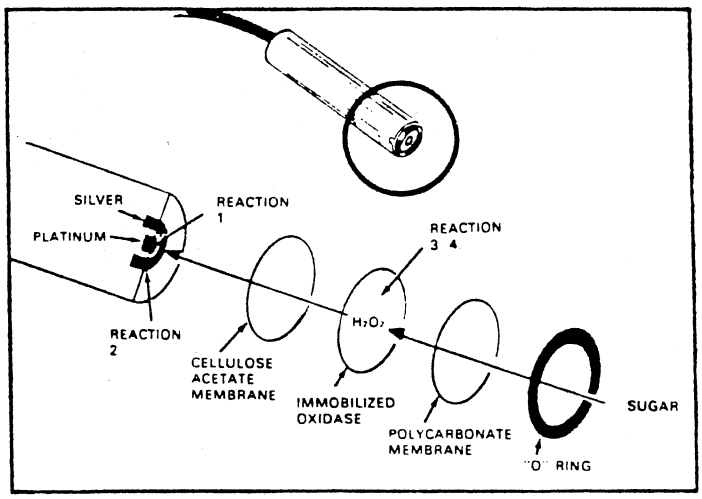

Figure 16. The YSI Industrial Analyzer sensor probe.

is approximately 5 microns thick, and has round pores of 0.03 microns diameter, small enough to exclude most unwanted enzymes from the reaction zone.

When glucose reaches the middle layer of the membrane, reaction 4 occurs almost instantaneously, producing hydrogen peroxide in proportion to the rate of arrival of glucose. A constant fraction of this hydrogen peroxide diffuses toward the platinum anode 1.

The anode is capable of oxidizing many other reducing agents in addition to hydrogen peroxide. To prevent reducing agents in the specimen from contributing to the sensor current, the membrane contains a third layer, which consists of cellulose acetate with a molecular weight cutoff of approximately 100. This final layer passes hydrogen peroxide readily, but excludes ascorbic acid and most other reducing agents common in foodstuffs. The probe signal current is therefore linearly proportional to the concentration of glucose in the sample chamber. A thermistor mounted on a disk of gold-plated silver in the temperature probe (see Figure 15) compensates for small fluctuations in sample temperature.

The YSI Model 27 is a semi-automated system. A sample is injected into the chamber with a syringe (25 microliters) when the ZERO/INJECT light is displayed on the panel. A WAIT instruction appears immediately and the digital display is blanked. After approximately 60 seconds, a READ instruction appears along with a locked numerical display of sugar concentration in milligrams per deciliter (1 dl = 100 ml). After the reading is noted, pressing the CLEAR button will blank the display and automatically flush the sample from the chamber. The WAIT instruction appears for approximately 35 seconds. At the end of this period, the ZERO/INJECT instruction again appears and the display is reactivated so that the reading can be observed and adjusted to zero if necessary. The instrument would now be ready for a new calibration solution or sample.

Enzymes

Robyt (1967) states that it is widely believed that alpha-amylases from a number of sources hydrolyze starch at random points in the polymer chain to give a random distribution of products that eventually become identical. Alpha-amylases cause hydrolysis of the interior alpha-(1-4) glucosidic bonds of amylose and amylopectin, and is thus an endo-hydrolase. McAllister (1979) reported that rupture can occur almost anywhere in a chain of alpha-(1-4) linked residues, so long as there are at least six D-glucosyl residues on one side, and at least three on the other side of the bond to be broken. Consequently the viscosity of gelatinous starch mashes is reduced. The final products of digestion of starch by alpha-amylases are soluble dextrin, glucose and maltose.

TAKA-THERM, a liquid bacterial alpha-amylase of

Bacillus lichentormis origin, produced by Miles Laboratories, Inc. was used in this experiment. Miles Laboratories Inc. (1980) state that TAKA-THERM exhibits exceptional thermostability and can liquify starches at temperatures above 90°C.

Whitaker (1972) defines gluco-amylase as an exo-splitting enzyme which removes glucose units consecutively from the non-reducing end of the substrate chains. The product of its action is glucose which clearly differentiates it from alpha and beta-amylases. Gluco-amylase hydrolyzes preferentially alpha-(1-4) linkages to give glucose but it can also hydrolyze alpha-(1-6) linkages at a much slower rate.

GASOLASE, a selected blend of enzymes derived mainly from Aspergillus niger and Rhizopus riveus, was also used in this experiment. Biocon Inc. (1980) states that GASOLASE incorporates alpha amylase, amyloglucosidase, protease, beta glucanase, cellulase, hemicellulase, pectinase, pantothenic acid, biotin, and a number of other essential vitamins and enzymes combined to give a complete system capable of dealing with the wide range of alcohol production conditions normally encountered in the ethanol production industry.

CHAPTER IV

EXPERIMENTAL PROCEDURES

Extruded grain products used in the fuel alcohol industry may increase to the overall production of the plant. Glucose production may be correlated with moisture content and temperature of the final extruded product. With these results, it can be determined if extruded grain products will significantly increase production of glucose from agricultural grains for conversion to alcohol.

The Insta-Pro 500 (described in Chapter III) is equipped with three thermocouples along the barrel. One was placed on each barrel segment to provide approximate temperatures for the entrance section, the transition zone, and the high temperature cooking zone. The orifice used on the exit section was a single hole orifice with a diameter of 0.5 inches. The orifice creates a restriction which can be varied by changing the distance between the end cone and the orifice (refer to Figure 11). The distance used in this experiment was determined by inspection of flow rate and degree of puffing. The orifice was adjusted to a position where flow of grain out of the extruder was uniform and a high degree of puffing is achieved. The actual distance from the orifice and the "degree" of puffing was not measured in these tests since the main objective in this adjustment was to achieve uniform flow.

Different steam lock configurations were used within the barrel to provide a variety of temperature profiles. This also, depending on the relative change of the steam locks, caused higher or lower shear rates combined with longer or shorter transition section lengths. The steam locks used (Figure 13) were numbered one (1) through four (4) for convenience. Number one (1) was the largest steam lock and number four (4) is the smallest. The diameters are 3.75 , 3.625 , 3.50 and 3.25 inches respectfully. Three different steam lock configurations were used in this study. They were configuration A, B, and C. Configuration A consisted of the largest steam lock (1) located at the metering section, the second largest (2) located at the front end of the transition zone, the third largest (3) located at the rear end of the transition zone, and the smallest (4) at the feed section. Configuration A therefore had steamlock order 1-2-3-4. Configurations B and C had steam lock orders of 1-2-2-3 and 2-2-3-4 respectfully.

The extruder was equipped with a water injection system that allowed metering of flow to be injected into the barrel. The system consisted of two pressure gauges combined with an orifice meter flow. Water flow rate as a function of pressure drop across the orifice was plotted in Figure 17. Knowing the initial moisture content of the grain, the product flow rate, and the flow rate of water

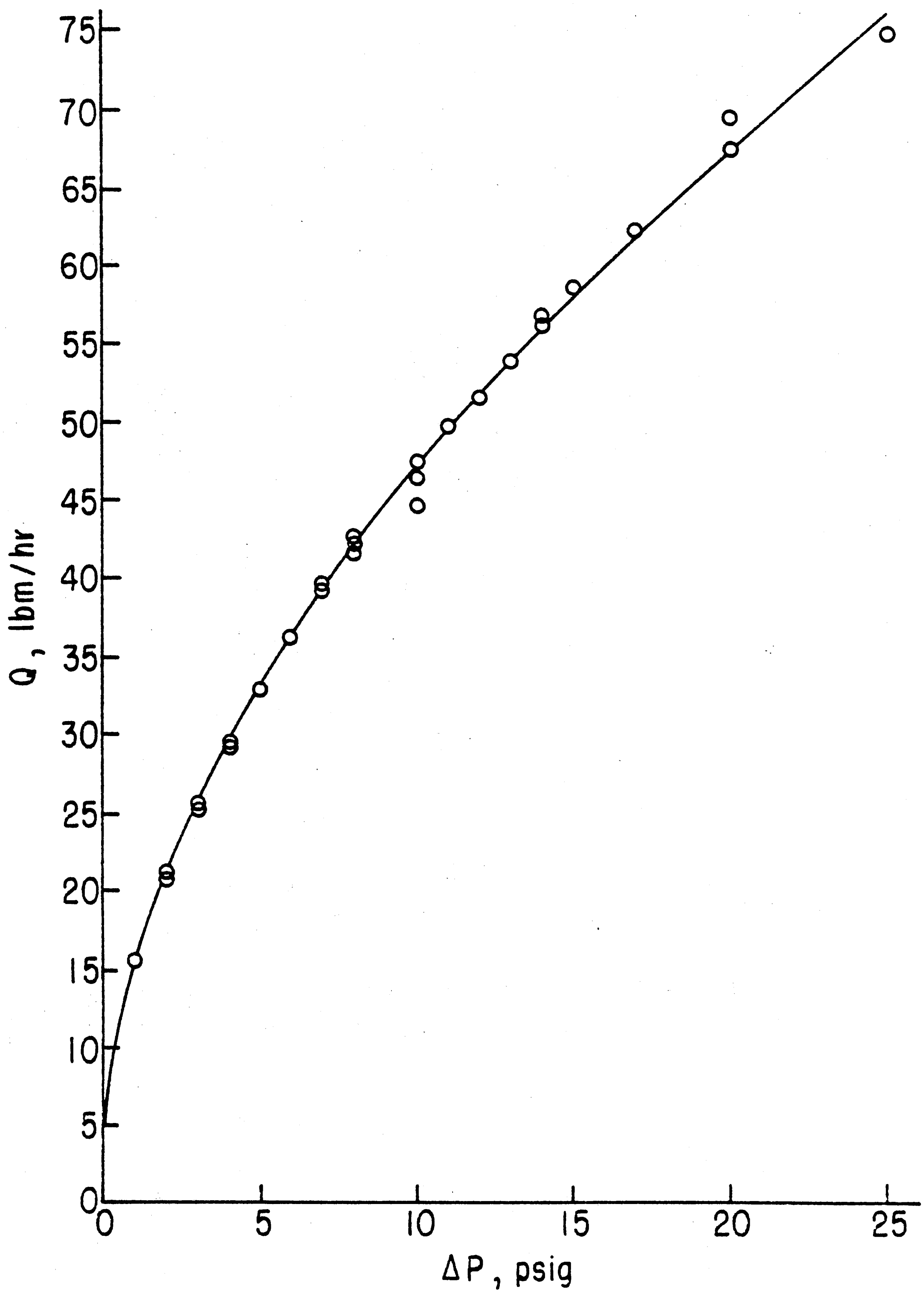

Figure 17. Indicated difference in pressure (psig) versus water flow rate (lbm/hr). For determination of grain moisture content in the extruder barrel.

through the water injection system, the moisture content inside the barrel was calculated. This addition of water is necessary to vary moisture content of grain entering the extruder. With some configurations, high temperatures may be achieved in the entrance section and result in causing a plug to form in the volumetric feeder. High temperatures could be controlled by using the water injection system.

The extruder was started with a continuous flow of soybeans from the vibratory feeder located above the barrel. The soybeans were used for start-up for two reasons. The first is that they have a high oil content which lubricated all the screw sections and barrel segments. The second purpose was to create a gradual increase in barrel temperature. Soybeans were easily extruded, therefore process conditions were not critical at this stage. When the temperature increased to approximately 220°F, grain was fed into the side of the barrel using the volumetric feeder. In this stage, grain was initially mixed with the soybeans in small increments. As grain mass flow rate was increased, the flow rate of soybeans was decreased until the vibratory feeder was shut off, discontinuing the addition of soybeans. The temperature increased rapidly with the steady decrease in soybean input. The addition of water was required while increasing the grain input to avoid extreme high temperatures, high shear rates, and to increase moisture content of the grain.

The extruder was operated at a uniform flow rate.

Water was added by regulating the pressure difference on the water injection system. To allow the extruder to come to equilibrium at this setting, a time period of 4 to 5 minutes was required. A sample was taken for a specified time interval and weighed to determine product flow rate. At the time the sample was taken, the three temperatures in the barrel are recorded. A small sample was taken immediately after the extruded grain left the orifice to determine approximate moisture content of the extruded product. The initial moisture content of the grain was determined using a Ohaus Moisture Balance. Pressure difference observed on the water injection system was recorded to determine the moisture content in the extruder barrel. Two samples of grain to be extruded were taken for determination of percent starch in the grain and for a batch cooked test. The extruded sample taken to specify flow rate was used for the extruded sample analysis.

To measure the glucose content in the samples, a YSI (Yellow Springs Instrument) Industrial Analyzer was used (described in Chapter III). This instrument is used due to its accuracy, speed, and convenience.

Enzyme rate tests were run to determine required concentration of enzymes needed and to determine time required for enzymes to convert the polysaccharides to glucose. Several tests were run with different dilution rates and different enzyme concentrations using extruded corn and extruded milo. Tests number 1 and number 2 (shown in

Appendix F) indicated that it is extremely important to sterilize all glassware and apparatus used in the test. Test number 1 was run with 0.5 grams of Gasolase and test number 2 was run with 1.0 grams gasolase. Both were run with extruded corn and showed that the maximum glucose value was achieved at approximately 60 minutes. The glucose value then started to descend, indicating contamination with competitive microorganisms. Tests number 3 and number 4 (shown in Appendix F) are repeats of number 1 and number 2 with all glassware and apparatus sterilized. These tests indicate no contamination and also that maximum glucose concentration was achieved at approximately 60 minutes using 0.5 grams or 1.0 grams of Gasolase. Test number 5 (shown in Appendix F) was run with extruded milo and 0.5 grams of Gasolase. Similarly, the test indicate 60 minutes was adequate time for the enzyme to break the bonds and produce glucose. The enzyme rate test procedures are outlined in Appendix B.

After results of these tests where inspected, it was determined that 0.5 gram of Gasolase enzyme with a 60 minute holding period would be used for extruded samples and that all glassware would be sterilized.

The procedures for determining starch content, starch conversion for extruded samples, and starch conversion for batch cooked samples are given in Appendixes C, D, and E respectfully. In the starch analysis (Appendix C), a dry sample of grain was used and the starch was solubilized using a ratio of 1.0 gram of dry sample mixed with 100 ml. of NaOH. Three grams of dry sample was used at this ratio to give a dry sample weight to NaOH ratio of 1,000 mg./dl. After adjustment of pH and addition of Gasolase, a portion of the sample was diluted 1:1 with water to give a dry sample weight to liquid volume ratio of 500 mg./dl. This dilution is necessary for convenience only. With the 500 mg./dl. ratio, the YSI 27 Industrial Analyzer may be calibrated to 200 mg/dl to read up to 500 mg/dl of glucose. The total glucose in the sample could then be calculated. The equation in step seven of the procedures (Appendix C) accounts for the change in the initial sample volume due to addition of Phosphoric acid. The YSI 27 reading was also multiplied by two to account for the 1:1 dilution with water. Percent of starch in the sample was the product of total glucose and 0.9. The multiplier 0.9 took into account the molecular weight fraction of water used when two glucose molecules are separated.

The extruded sample analysis (Appendix D) was similar to the starch analysis. The two main differences were that water was used at a 1:200 dilution ratio instead of NaOH and only 1/2 gram of Gasolase was used at a 60 minute holding time rather than 2 grams overnight. The percent starch conversion could then be calculated.

In the batch cooked sample analysis (Appendix E), 90.0 grams of grain are mixed with 300 ml. of water (equivalent to 22 gallons per bushel). A small quantity of Calcium

Chloride or Calcium Oxide is added for nutritional requirements. TAKA-THERM was added in a quantity equal to 22.5 grams per bushel. The sample was then held at 200°F for 90 minutes. After cooking, a dilution was made with water to bring the total dry sample weight water ratio to 500 mg/dl. Gasolase was added at near 100°F and held for 60 minutes. The total glucose was determined in the same manner as in the starch analysis procedure. The percent starch conversion could then be calculated.

Table I shows the experimental design for extruding corn and milo. Procedures for determining the starch to glucose conversion are given in Appendix D. Procedures for determination of background starch and batch cooked sample analysis are given in Appendices C and E respectfully.

TABLE I

EXPERIMENTAL DESIGN FOR
EXTRUDED PRODUCTS

GRAIN TYPE	SCREW CONFIGURATION	EXTRUSION MOISTURE CONTENT	BARREL TEMPERATURES	FLOW RATE	STARCH TO GLUCOSE CONVERSION
CORN	A	18 ↓ 22	measure	measure	calculate
	B	18 ↓ 22	measure	measure	calculate
	C	18 ↓ 22	measure	measure	calculate
MILO	A	19 ↓ 23	measure	measure	calculate
	B	19 ↓ 23	measure	measure	calculate
	C	19 ↓ 23	measure	measure	calculate

CHAPTER V

RESULTS AND DISCUSSION

The results of all extruded grain tests are tabulated in Appendix G. The percent of starch conversion were the dependent variable in all analysis in this chapter. Independent variables were:

T_1 = average exit temperature

T_2 = average transition zone temperature (°F)

T_3 = average entrance section temperature (°F)

R_1 = temperature gradient for forward section of extruder barrel (°F/inch)

R_2 = temperature gradient for rear section of extuder barrel (°F/inch)

m_p = product flow rate (dry basis - lbm/hr)

S_e = starch conversion in extruded sample (%)

MC_e = extrusion moisture content (wet basis - %)

T_f = fractional part of the total temperature change in the extruder barrel (°F)

The Insta-Pro 500 is an autogenous extruder and, therefore, all energy addition comes from viscous dissipation of the mechanical drive energy.

Temperature profiles for the experiments are shown in Figures 18 through 23. They were all run at approximately 20 KW power consumption on the Insta-Pro extruder. These figures show the range of temperature profiles for each screw configuration and type of grain. For ground corn (Figures 18, 19, and 20), steam lock configuration A (Figure 18) yielded greater consistency in results due to the narrow band of temperature profiles. This shows that a change of moisture content or product flow rate when using steam lock configuration A did not affect the final cooking temperature as much as other configurations. It also can be seen from Figure 18 that the average temperature gradient was constant from the feed section to the metering section. Figures 19 and 20 (steam lock configurations B and C respectfully) have considerably wider bands of temperature profiles. This shows that a change in moisture content caused significantly different temperature profiles. These figures also show that as the grain passed through the transition zone the temperature gradient increased.

Figures 21, 22, and 23 show the temperature profiles for ground milo. Steam lock configuration A (Figure 21) shows a narrow band of temperature profiles indicating small changes in the profiles due to moisture content.

Figure 22 shows the temperature profiles for steam lock configuration B. The wide band indicates changes in moisture content and flow rate cause significant changes in

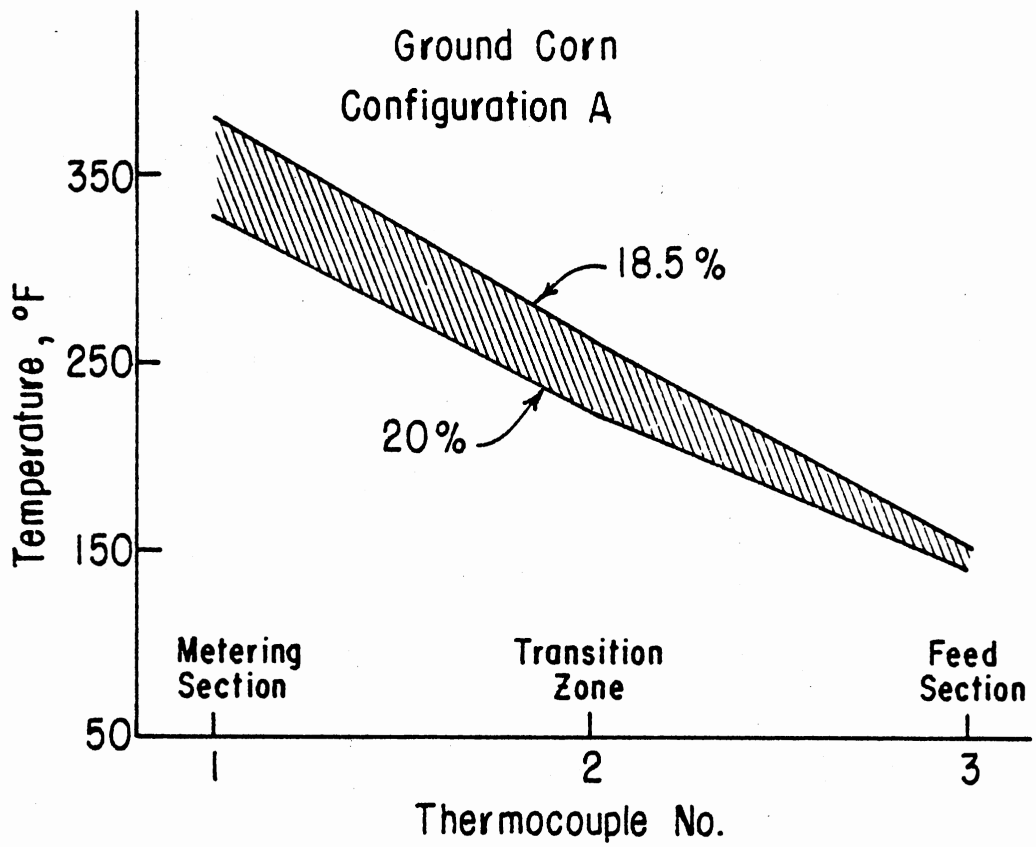

Figure 18. Temperature profile for ground corn run with steam lock configuration A and with moisture content ranging from 18.5 to 20 %.

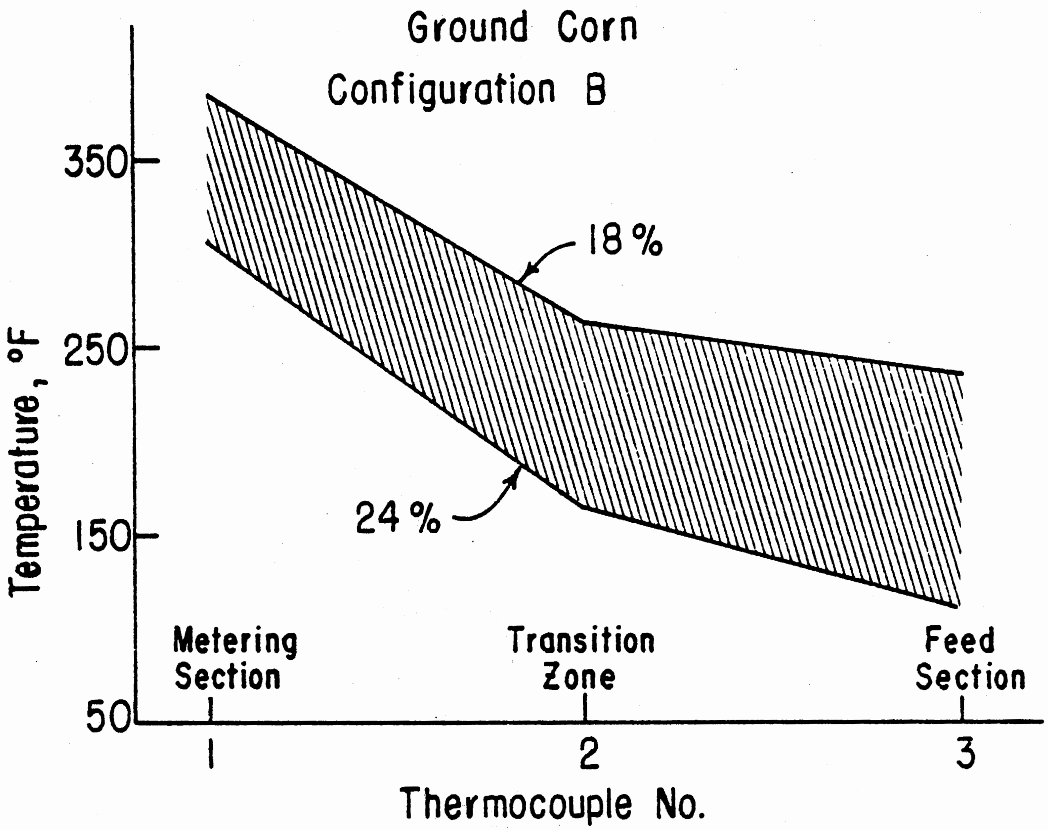

Figure 19. Temperature profile for ground corn run with steam lock configuration B and with moisture content ranging from 18 to 24 %.

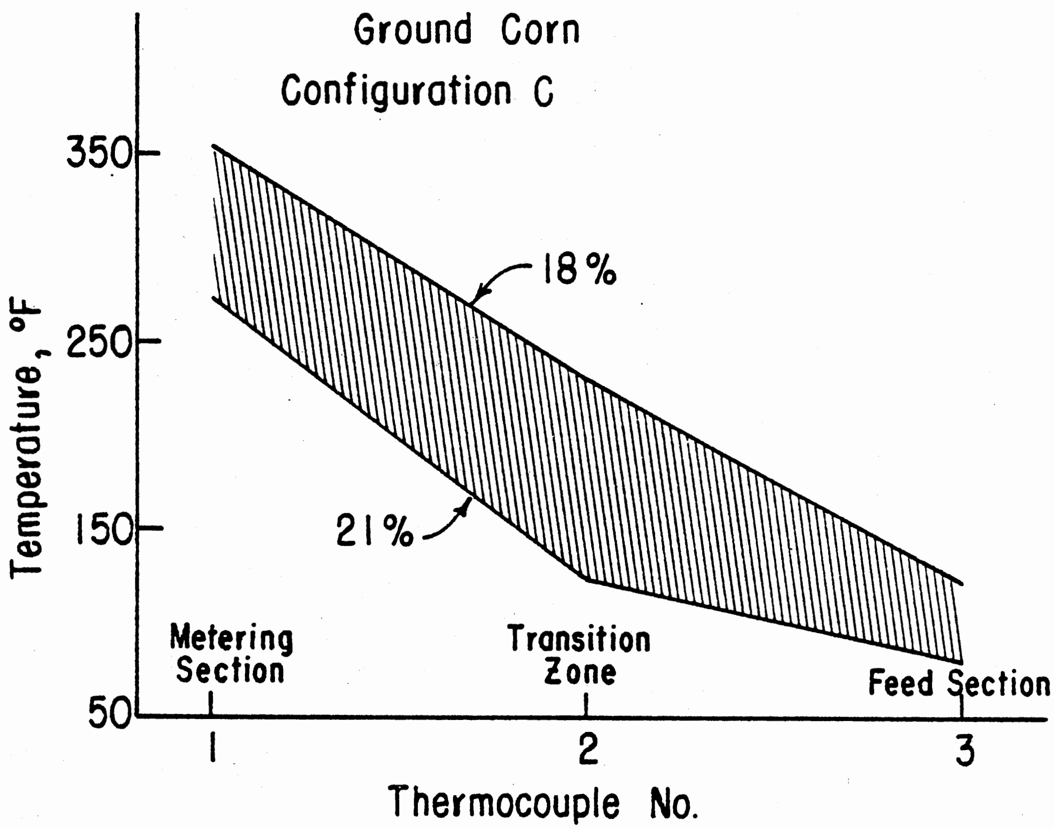

Figure 20. Temperature profile for ground corn run with steam lock configuration C and with moisture content ranging from 18 to 21 %.

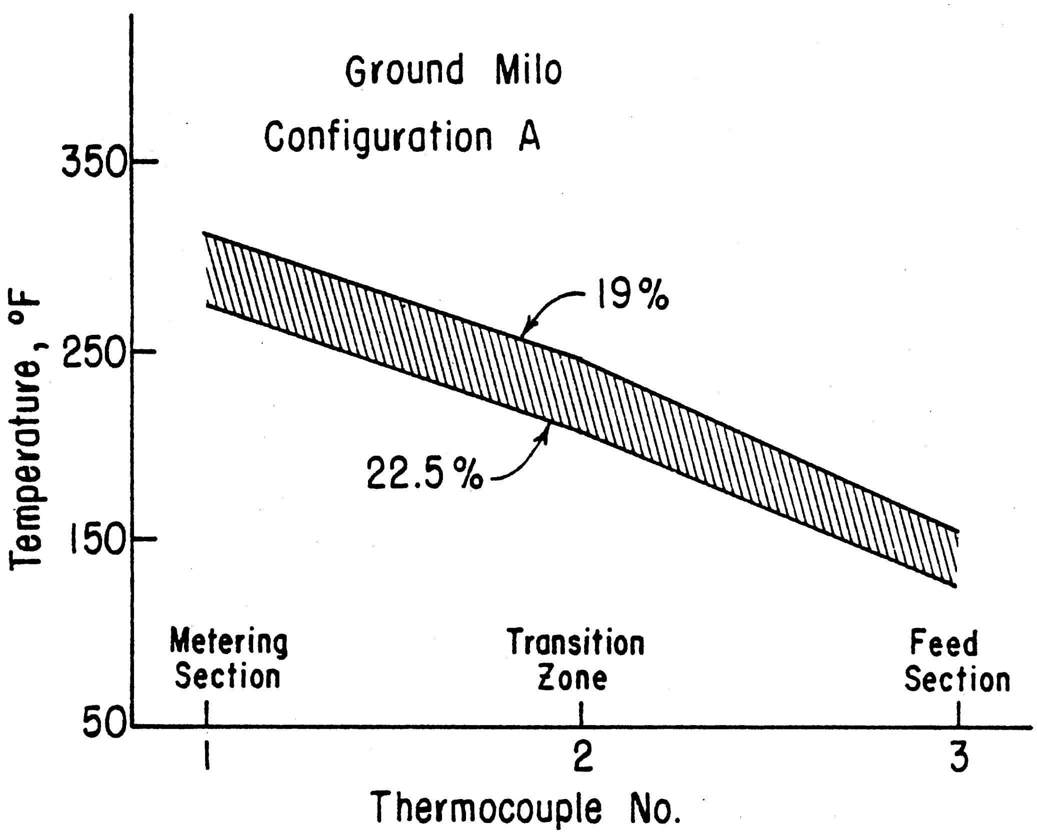

Figure 21. Temperature profile for ground milo run with steam lock configuration A and with moisture content ranging from 19 to 22.5 %.

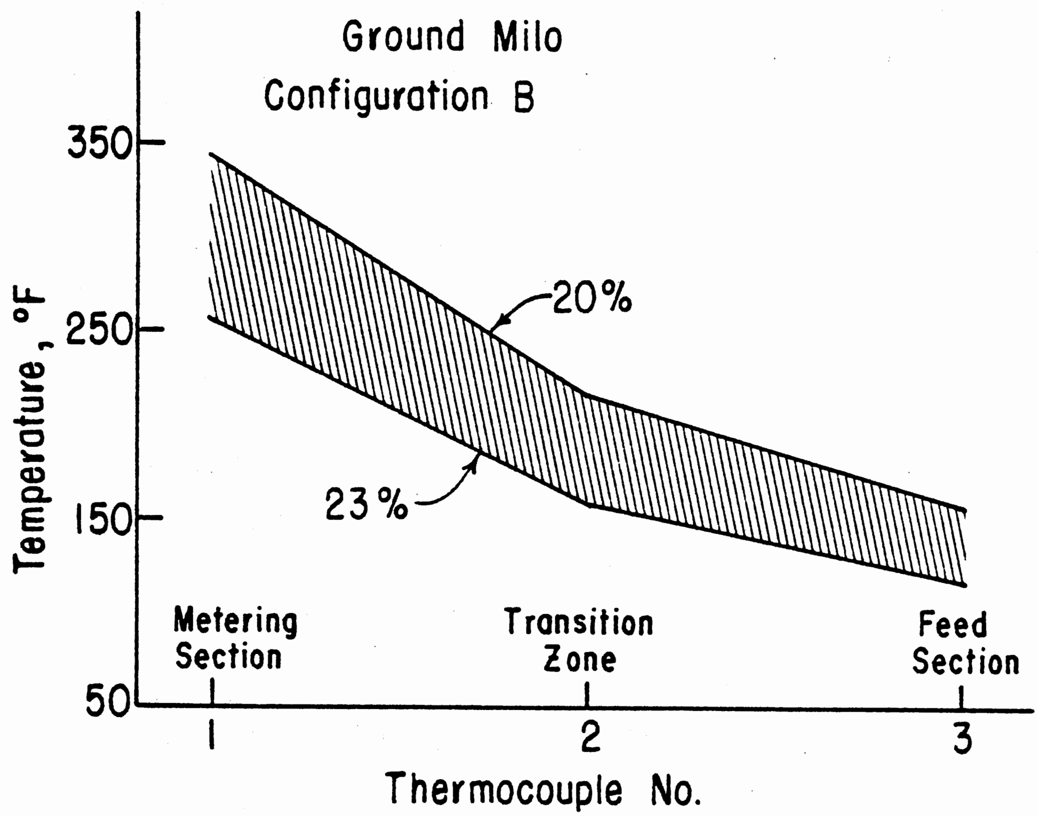

Figure 22. Temperature profile for ground milo run with steam lock configuration B and with moisture content ranging from 20 to 23 %.

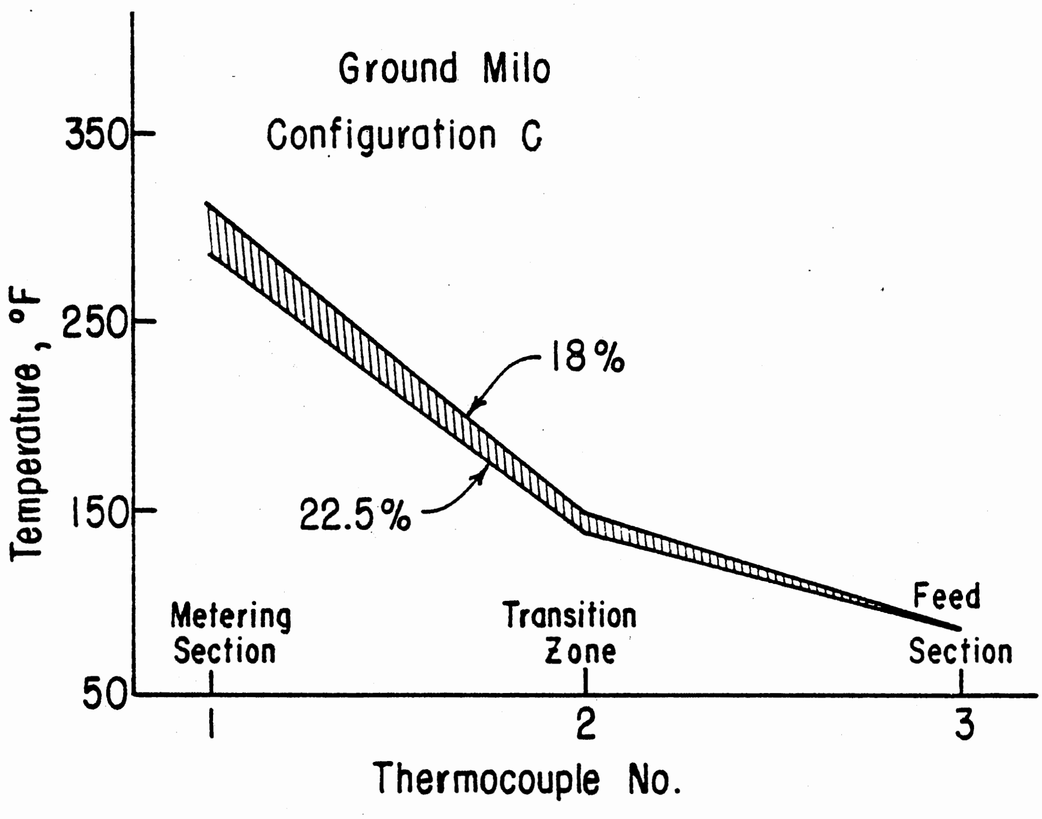

Figure 23. Temperature profile for ground milo run with steam lock configuration C and with moisture content ranging from 18 to 22.5 %.

cooking characteristics. The temperature gradient also increases through the transition zone. Figure 23 shows the temperature profiles for steam lock configuration C. The narrow band indicates that a change in moisture content or product flow rate causes little change in the temperature profile. The temperature gradient increased rapidly through the transition zone, as shown in the Figure 23.

Changes in performance caused by changing steam lock configurations were due to differences in shear rate. The shear rate in the extruder barrel may be increased or decreased depending on the steam lock configuration. Increased shear caused a higher mechanical dissipation of energy to the grain, which disrupted the starch cell. This increased availability of amylopectin for enzyme attack.

The effects of extrusion cooking temperature on conversion of corn starch to glucose is shown in Figure 24. Results of batch cooked tests and background starch analysis tests are also included in this plot. As shown in the plot, extrusion cooking did not produce good cooking characteristics at exit temperatures below 328°F. The batch cooked samples consistently produced more glucose than did the extruded samples run at exit temperatures below 328°F. This was because of the small amount of gelatinization occur at low extrusion temperatures. As extrusion temperature increased, glucose converted from enzymatic reactions in these samples started to exceed glucose produced in batch cooked processes. At high extrusion

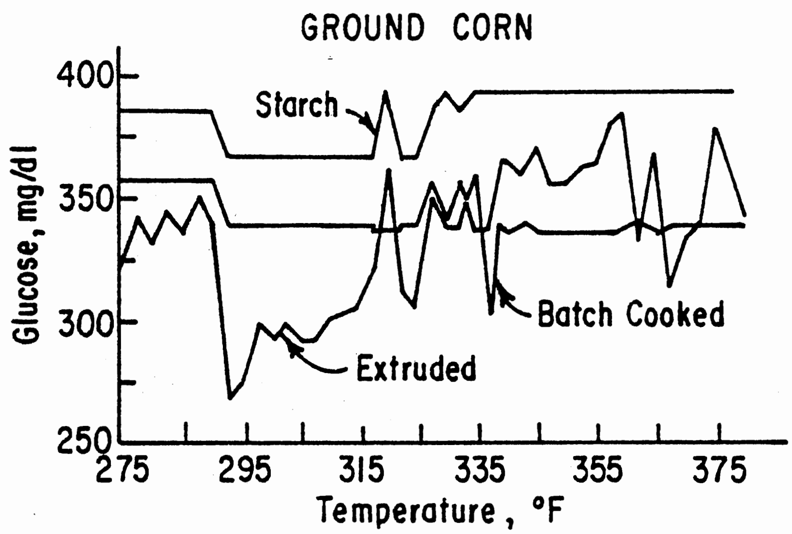

Figure 24. Effect of increasing discharge temperature on conversion of corn starch to glucose.

temperatures, extrusion cooking converted a significantly higher proportion of starch to glucose than the batch cooking procedure. This effect was due to increased gelatinization of starch at higher temperatures. This allowed enzymes to readily break the alpha-(1-4) bonds. At lower gelatinization, these bonds were not accessible to the enzymes.

The effects of extrusion cooking temperature on conversion of milo starch to glucose is shown in Figure 25. Results of batch cooked tests and background starch analysis tests are also included in this plot. At exit temperatures below 293°F, the batch cooked tests consistently produced a higher percentage of glucose than did extrusion cooking. As the extrusion temperature increased, extrusion cooking started to produce higher glucose concentrations when compared to conventional batch cooking. Because of the nature of milo starch, it was not possible to reach temperatures as high as those for corn without burning the product. Figures 24 and 25 show that increased extrusion temperatures resulted in significant increases in conversion of starch to glucose. The exit temperature where extrusion cooking starts to convert a higher proportion of starch to glucose than the batch cooking procedure was different for corn and milo (293°F for milo and 328°F for corn). This was due to a higher percentage of amylopectin in milo than in corn. Milo starch, due to more amylopectin, absorbed a greater amount of water. This caused the milo starch to

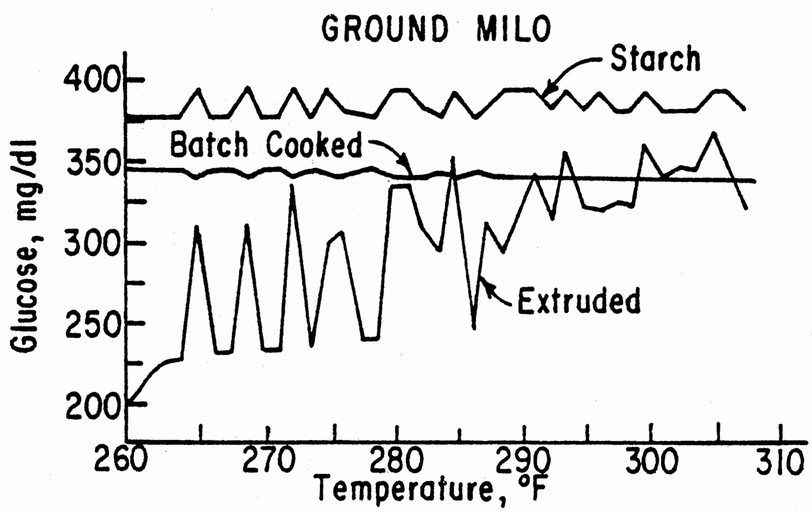

Figure 25. Effect of increasing discharge temperature on conversion of milo starch to glucose.

swell and rupture at lower temperatures than corn starch.

Figure 26 shows that for extrusion temperature, for corn starch above 363°F extrusion cooking resulted in higher conversion rates of starch to glucose. Tests 5 through 14 (identified in Appendix 6) were run with ground on at temperatures from 363°F to 380°F. The average increase in efficiency due to extrusion cooking was 8.1 percent.

The effect of discharge temperature on starch conversion for all ground corn samples is shown in Figure 27. The linear regression analysis computations are shown in Table II. The coefficient of correlation, 0.3621, is a relative measure of the association between the discharge temperature and starch conversion. It can vary from minus one (which indicates perfect negative correlation) to one (which indicates perfect positive correlation). The coefficient of determination, 0.1311,(the square of the correlation coefficient) is the ratio of the variation explained by the regression line over the total variation of the data. Therefore, the model indicates that the regression line with the intercept of 64.357 and a slope of 0.060 explains 13.11 percent of the total variation of the data points.

The sampling distribution used for testing the hypothesis that the slope is equal to zero is the F-distribution. Assuming a confidence level of 95 percent, this indicates whether the overall regression equation is

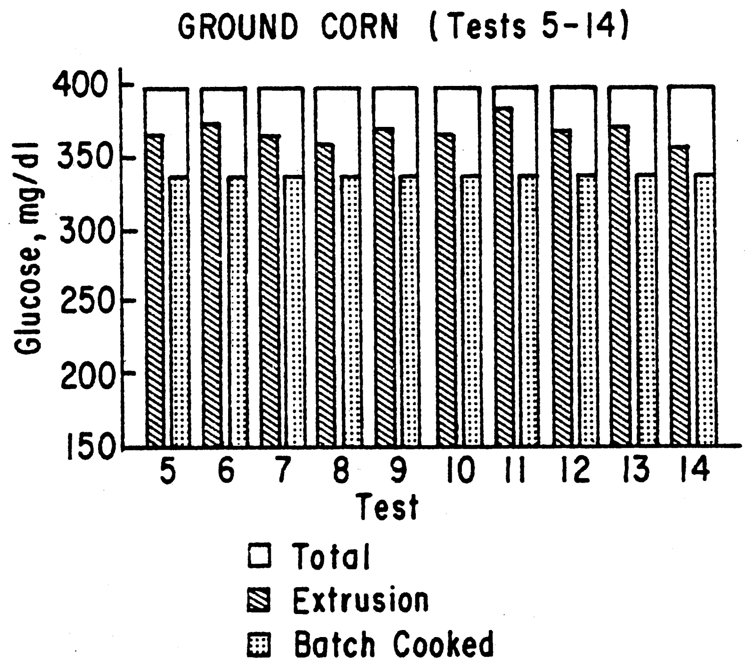

Figure 26. Starch conversion efficiency for ground corn extruded at high temperatures (tests are identified in Appendix G).

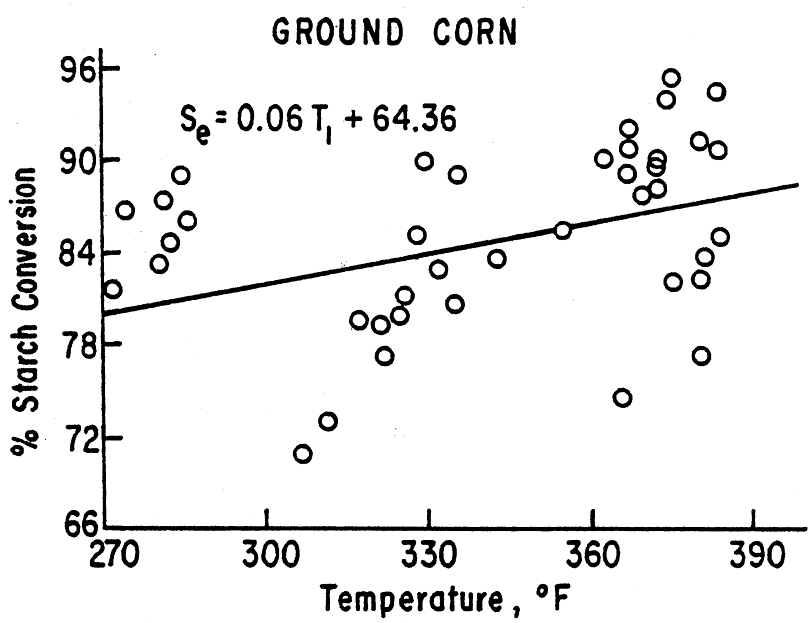

Figure 27. Effect of discharge temperature on starch conversion of extruded ground corn.

TABLE II

ANALYSIS OF VARIANCE OF STARCH CONVERSION AND EXIT TEMPERATURE FOR ALL GROUND CORN

DEPENDENT VARIABLE: S_e

SOURCE	DF	SUM OF SQUARES	MEAN SQUARE	F VALUE	PR>F	R-SQR
T_1	1	189.924	189.924	6.19	0.0170	0.131
ERROR	41	1258.310	30.690			
TOTAL	42	1448.234				C.V.=6.545

PARAMETER	ESTIMATE	STD ERROR OF ESTIMATE
INTERCEPT	64.357	8.200
T_1	0.060	0.024

statistically significant. In this case of simple regression, the T-test and the F-test are equivalent since there is only one independent variable. The probability that F-calculated is greater than the F-distribution for this model is equal to 0.017. Assuming a 98% confidence level, the conclusion is that the regression equation

$$S_e = 64.36 + 0.060(T_1) \qquad (1)$$

where S_e = starch conversion (%)

T_1 = exit temperature (°F)

will be better than the mean as a method of forecasting. However, the data shows that exit temperature has little effect on corn starch gelatinization during extrusion cooking due to the low coefficient of determination.

As stated previously, the model equation explains only 13.11 percent of the total variation of the data. Linear analysis for this set of data isolated by steam lock configurations are shown in Tables III, IV, and V. In Table III (configuration B), the probability that F-calculated is greater than the F-distribution for the model equation of $S_e = 35.43 + 0.134(T_1)$ is 0.001. This indicates that the regression equation will be better than the mean as a method of forecasting. The coefficient of determination value indicates that 38.2 percent of the variation is explained by the model. This value is still low, indicating that discharge temperature is not highly correlated with corn starch conversion. In Tables IV and V

TABLE III

ANALYSIS OF VARIANCE OF STARCH CONVERSION AND EXIT TEMPERATURE FOR GROUND CORN AND CONFIGURATION B

DEPENDENT VARIABLE: S_e

SOURCE	DF	SUM OF SQUARES	MEAN SQUARE	F VALUE	PR>F	R-SQR
T_1	1	322.633	322.633	13.63	0.0013	0.382
ERROR	22	520.854	23.675			
TOTAL	23	843.487			C.V.=5.947	

PARAMETER	ESTIMATE	STR ERROR OF ESTIMATE
INTERCEPT	35.432	12.605
T_1	0.134	0.036

TABLE IV

ANALYSIS OF VARIANCE OF STARCH CONVERSION AND EXIT TEMPERATURE FOR GROUND CORN AND CONFIGURATION A

DEPENDENT VARIABLE: S_e

SOURCE	DF	SUM OF SQUARES	MEAN SQUARE	F VALUE	PR>F	R-SQR
T_1	1	0.655	0.655	0.18	0.6831	0.022
ERROR	8	29.215	3.652			
TOTAL	9	29.870			C.V.=2.116	

PARAMETER	ESTIMATE	STR ERROR OF ESTIMATE
INTERCEPT	83.176	16.892
T_1	0.019	0.046

TABLE V

ANALYSIS OF VARIANCE OF STARCH CONVERSION AND EXIT TEMPERATURE FOR GROUND CORN AND CONFIGURATION C

DEPENDENT VARIABLE: S_e

SOURCE	DF	SUM OF SQUARES	MEAN SQUARE	F VALUE	PR>F	R-SQR
T_1	1	4.608	4.608	0.76	0.4132	0.095
ERROR	7	42.634	6.091			
TOTAL	8	47.242			C.V.=2.874	

PARAMETER	ESTIMATE	STD ERROR OF ESTIMATE
INTERCEPT	78.331	8.716
T_1	0.026	0.029

(configurations A and C respectfully), the F-calculated values are low. Therefore the hypothesis that the slope is equal to zero cannot be rejected. The probable cause of low F-calculated values is due to small sample size for steam lock configurations A and C.

The effect of exit temperature on starch conversion for all ground milo samples is shown in Figure 28. As with ground corn samples, this plot shows an increase in starch conversion as extrusion temperature increased. The linear regression analysis for this data is given in Table VI. The coefficient of determination is equal to 0.661. The probability that F-calculated is greater than F-distribution for this model is equal to 0.0001. The null hypothesis can not be rejected at the confidence level of 99 percent. The model equation selected is:

$$S_e = -116.27 + 0.657\ (T_1) \qquad (2)$$

where S_e = starch conversion (%)

T_1 = exit temperature (°F)

The data shows that exit temperature had a significant effect on milo starch gelatinization. It was expected that an increase in exit temperature would increase the milo starch conversion. Unlike tests run with ground corn, ground milo data have a higher coefficient of determination. This effect is related to the higher percentage of amylopectin in milo starch than in corn starch (as explained earlier) in the coefficient of determination.

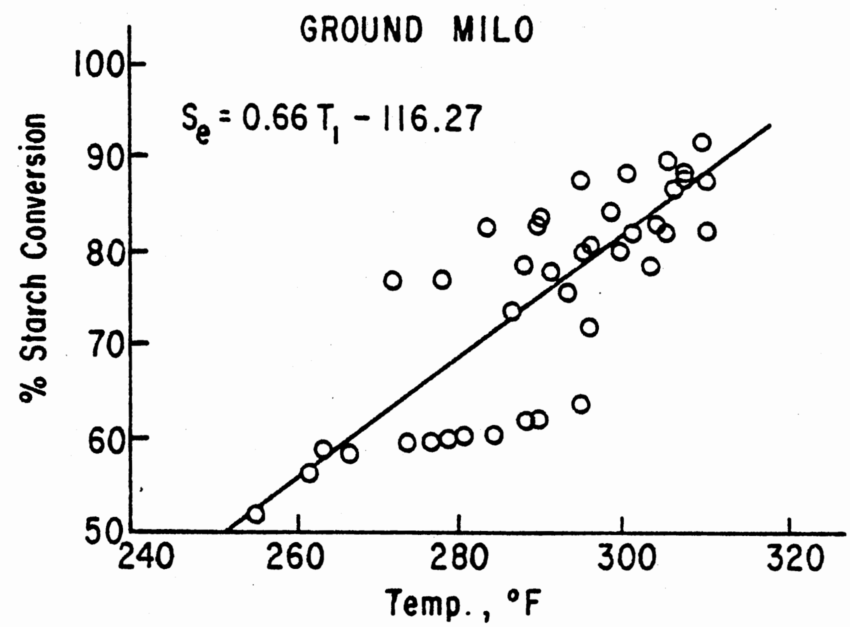

Figure 28. Effect of discharge temperature on starch conversion of extruded ground milo.

TABLE VI

ANALYSIS OF VARIANCE OF STARCH CONVERSION AND EXIT TEMPERATURE FOR ALL GROUND MILO

DEPENDENT VARIABLE: S_e

SOURCE	DF	SUM OF SQUARES	MEAN SQUARE	F VALUE	PR>F	R-SQR
T_1	1	3387.302	3387.302	72.22	0.0001	0.661
ERROR	37	1735.430	46.903			
TOTAL	38	5122.732			C.V.=9.128	

PARAMETER	ESTIMATE	STD ERROR OF ESTIMATE
INTERCEPT	-116.274	22.538
T_1	0.657	0.077

Effect of moisture content on conversion of corn starch to glucose by extrusion cooking is shown in Figure 29. The linear regression analysis computations for this data are given in Table VII. The coefficient of determination value of 0.695 indicates that the regression line with an intercept of 153.78 percent and a slope of -3.44 explains 69.50 percent of the total variation of the data points. The probability that F-calculated is greater than F-distribution for this model is equal to 0.0001. This specifies that the hypothesis of the slope being equal to zero may be rejected assuming a 99 percent confidence interval. The mathematical model describing the data in Figure 29 is:

$$S_e = 153.78 - 3.44\ (MC_e) \qquad (3)$$

where: S_e = starch conversion (%)

MC_e = extrusion moisture content (%)

The model equation shows that as extrusion moisture content increased, starch to glucose conversion decreased. The increase in moisture content caused lower temperatures in the extruder barrel and resulted in less gelatinization of the corn starch.

Effect of extrusion moisture content on conversion of milo starch to glucose by extrusion cooking is shown in Figure 30. The linear regression analysis computations for this data are given in Table VIII. The coefficient of determination value of 0.162 shows that the regression line

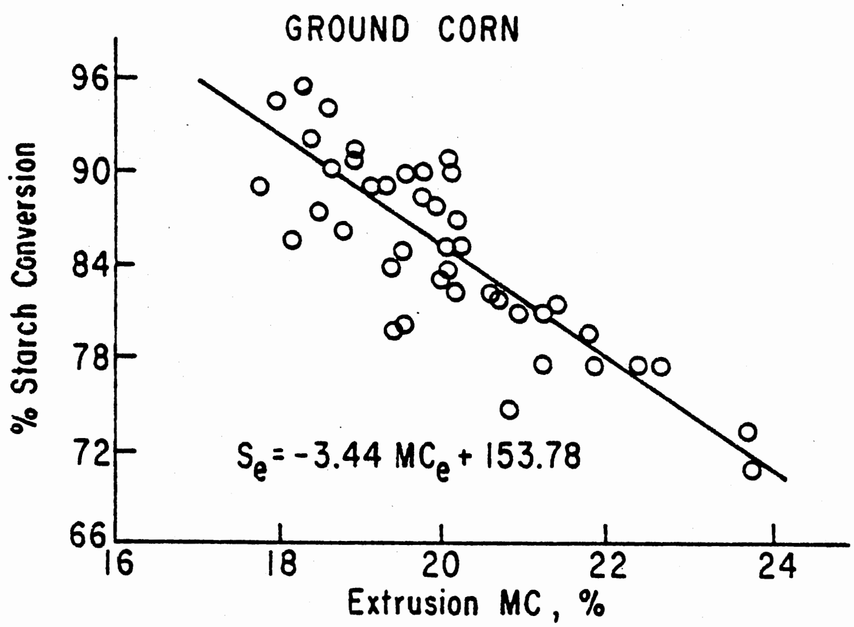

Figure 29. Effect of extrusion moisture content on starch conversion of extruded ground corn.

TABLE VII

ANALYSIS OF VARIANCE OF STARCH CONVERSION AND EXTRUSION MOISTURE CONTENT FOR ALL GROUND CORN

DEPENDENT VARIABLE: S_e

SOURCE	DF	SUM OF SQUARES	MEAN SQUARE	F VALUE	PR>F	R-SQR
MC_e	1	1006.462	1006.462	93.41	0.0001	0.695
ERROR	41	441.772	10.775			
TOTAL	42	1448.234				C.V.=3.878

PARAMETER	ESTIMATE	STD ERROR OF ESTIMATE
INTERCEPT	153.783	7.171
MC_e	-3.437	0.356

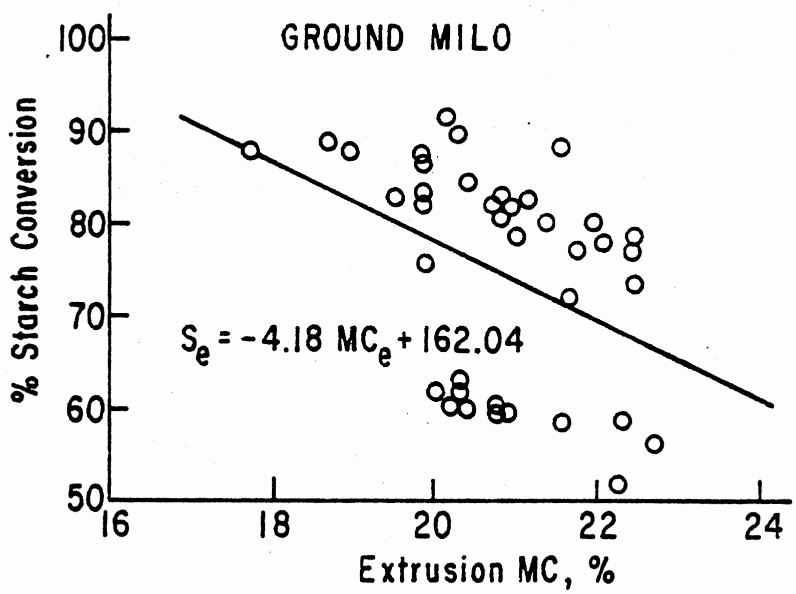

Figure 30. Effect of extrusion moisture content on starch conversion of extruded ground milo.

TABLE VIII

ANALYSIS OF VARIANCE OF STARCH CONVERSION AND EXTRUSION MOISTURE CONTENT FOR ALL GROUND MILO

DEPENDENT VARIABLE: S_e

SOURCE	DF	SUM OF SQUARES	MEAN SQUARE	F VALUE	PR>F	R-SQR
MC_e	1	828.951	828.951	7.14	0.0111	0.162
ERROR	37	4293.781	116.048			
TOTAL	38	5122.732				C.V.=14.358

PARAMETER	ESTIMATE	STR ERROR OF ESTIMATE
INTERCEPT	162.044	32.603
MC_e	-4.176	1.562

with the intercept of 162.04 and a slope of -4.18 explains 16.18 percent of the total variation of the data points. A comparison of this analysis to that of corn starch shows that there is a significant lack of fit for milo starch. This shows that gelatinization of milo starch was not the same as gelatinization of corn starch. While the corn starch could be modeled to account for 69.50 percent of the variation, the milo starch account for only 16.18 percent of the variation in the data. The probability that F-calculated is greater than the F-distribution for this model is 0.011. The null hypothesis is rejected and the model equation shown in Figure 30:

$$S_e = 162.04 - 4.18\ (MC_e) \tag{4}$$

where: S_e = starch conversion (%)

MC_e = extrusion moisture content (%)

Therefore, the data shows that as extrusion moisture content increased, milo starch conversion decreased. Moisture content may be decreased to approximately 18 percent with ground milo. At this level, burning of the product occurred which caused a rapid decrease in starch. This was caused by the increased shear on the product as moisture decreases. The shear rate in the barrel may also be increased or decreased by changing the steam lock configuration. This increases mixing and mechanical energy dissipation.

Effect of product flow rate on corn starch conversion is shown in Figure 31. The linear regression analysis computations are shown in Table IX. The coefficient of determination value of 0.008 indicates that the regression line with the intercept of 80.01 and slope of 0.01 explains only 0.80 percent of the total variation of the data points. The probability that F-calculated is greater than F-distribution for this model is 0.566. The null hypothesis can not be rejected at the confidence level of 95 percent. The model equation shown in Figure 31 is:

$$S_e = 80.01 + 0.01\ (m_p) \qquad (5)$$

where: S_e = starch conversion (%)

m_p = product flow rate (lbm/hr)

Effect of product flow rate on milo starch conversion is shown in Figure 32. The linear regression analysis computations are shown in Table X. The coefficient of determination value 0.533 indicates the model equation

$$S_e = 152.66 - 0.19\ (m_p) \qquad (6)$$

where: S_e = starch conversion (%)

m_p = product flow rate (lbm/hr)

explains 53.3 percent of the total variation of the data points. The probability that F-calculated is greater than F-distribution for this model is 0.001. The null hypothesis can be reqected at the level of 99 percent. Therefore, the data showed that decreased flow rates increased milo starch conversion. Cause of increased conversion at lower

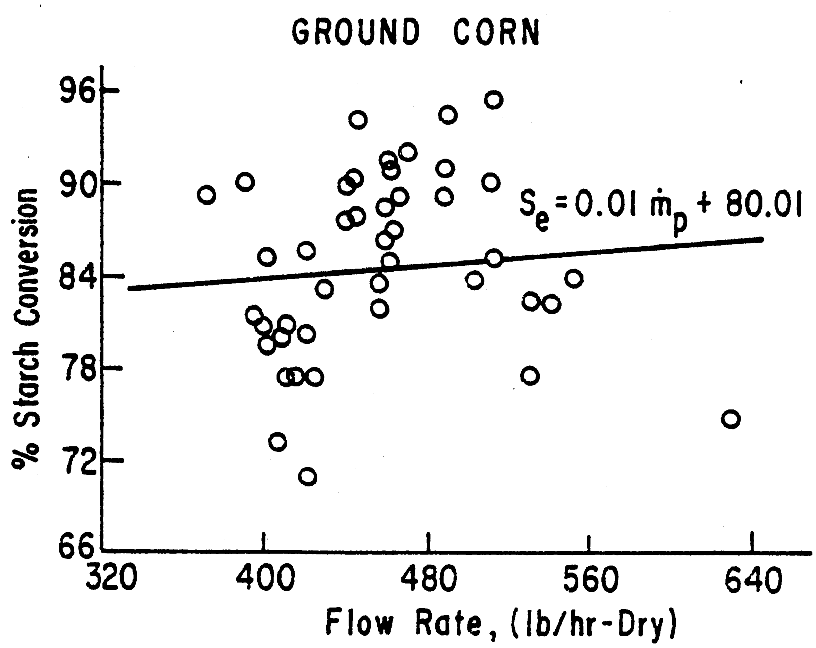

Figure 31. Effect of extruder flow rate on starch conversion of extruded ground corn.

TABLE IX

ANALYSIS OF VARIANCE OF STARCH CONVERSION AND EXTRUDER PRODUCT FLOW RATE FOR ALL GROUND CORN

DEPENDENT VARIABLE: S_e

SOURCE	DF	SUM OF SQUARES	MEAN SQUARE	F VALUE	PR>F	R-SQR
$\dot{m}_p$	1	11.740	11.740	0.34	0.5659	0.008
ERROR	41	1436.494	35.036			
TOTAL	42	1448.234			C.V.=6.992	

PARAMETER	ESTIMATE	STD ERROR OF ESTIMATE
INTERCEPT	80.012	8.059
$\dot{m}_p$	0.010	0.017

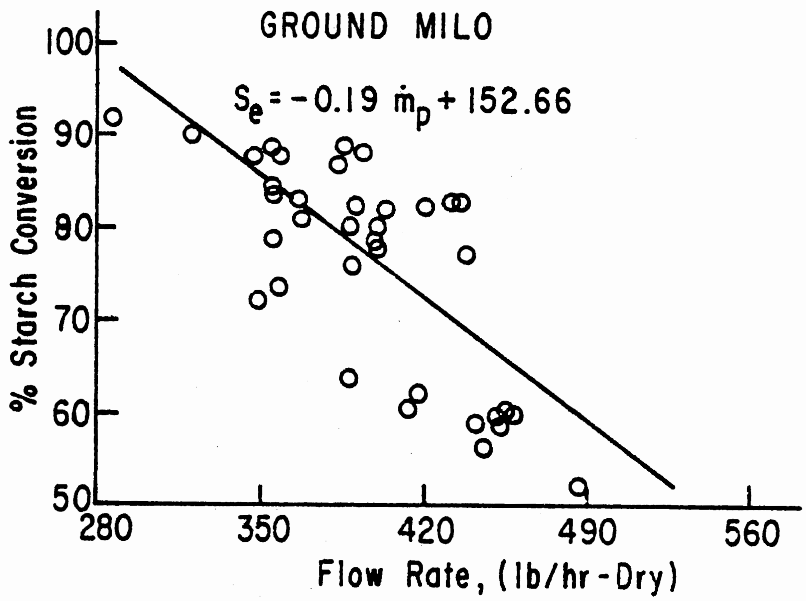

Figure 32. Effect of extruder flow rate on starch conversion of extruded ground milo.

TABLE X

ANALYSIS OF VARIANCE OF STARCH CONVERSION AND EXTRUDER PRODUCT FLOW RATE FOR ALL GROUND MILO

DEPENDENT VARIABLE: S_e

SOURCE	DF	SUM OF SQUARES	MEAN SQUARE	F VALUE	PR>F	R-SQR
$\dot{m}_p$	1	2731.011	2731.011	42.25	0.0001	0.533
ERROR	37	2391.721	64.641			
TOTAL	38	5122.732			C.V.=10.716	

PARAMETER	ESTIMATE	STD ERROR OF ESTIMATE
INTERCEPT	152.656	12.012
$\dot{m}_p$	-0.194	0.030

flow rates was associated with increased residence time. The analysis for milo starch explains more variation of the data than the analysis for corn starch. Corn starch did not significantly depend on resident time for gelatinization. Milo starch depended on this resident time, which increased starch conversion rate. This was reasonable to expect since milo starch uses this residence time to absorb water and thereby rupture the starch cells at lower temperature than corn starch. Corn starch depended more on high temperatures and high shear rates for cell rupture due to its lower amylopectin content.

A stepwise regression procedure for analysis of corn starch is shown in Table XI. The dependent variable S_e and independent variables T_1, T_2, T_3, R_1, R_2, m_p, MC_e, and T_f are used in the model. In the stepwise method, variables are added one by one to the model. The chosen level of F-statistic for a variable to be added was at the 85 percent level of significance. After a variable was added, the stepwise method looked at all the variables already included in the model and deleted any variable that did not produce an F-statistic significant at the 85 percent level. Only after this check was made and the necessary deletions accomplished can another variable added to the model. The stepwise process ended when none of the variables outside the model had an F-statistic significant at the 85 percent level. Step one of the analysis showed that extrusion moisture content was the most significant variable, explaining 69.50

TABLE XI

STEPWISE REGRESSION PROCEDURE
FOR DEPENDENT VARIABLE S_e
(GROUND CORN)

STEP 1 VARIABLE MC_e ENTERED

SOURCE	DF	SUM OF SQUARES	MEAN SQUARE	F VALUE	PR>F	R-SQR
MC_e	1	1006.462	1006.462	93.41	0.0001	0.695
ERROR	41	441.772	10.775			
TOTAL	42	1448.234				

PARAMETER	ESTIMATE	STD ERROR	TYPE II SS	F VALUE	PR>F
INTERCEPT	153.783				
MC_e	-3.437	0.356	1006.46	93.41	0.0001

STEP 2 VARIABLE R_1 ENTERED

SOURCE	DF	SUM OF SQUARES	MEAN SQUARE	F VALUE	PR>F	R-SQR
MC_e & R_1	2	1095.242	547.621	62.05	0.0001	0.756
ERROR	40	352.992	8.825			
TOTAL	42	1448.234				

PARAMETER	ESTIMATE	STD ERROR	TYPE II SS	F VALUE	PR>F
INTERCEPT	158.711				
MC_e	-3.023	0.347	668.781	75.78	0.0001
R_1	-0.586	0.185	88.780	10.06	0.0029

percent of the total variation of the data. Step two added the temperature gradient for the forward section of the extruder barrel. This increased the explained variation in the data to 75.63 percent. Both of the F-statistics in this model meet a significance level of 99 percent. The model indicated that a significant part of total gelatinization took place in the forward end (metering and transition zones) of the barrel. As the temperature gradient increased in this section, starch conversion increased. As moisture content within the extruder barrel increased, starch conversion decreased. Moisture content was the most highly correlated variable. This was due to the increased shear on the grain as moisture decreased. The analysis showed that all other variables did not meet the 85 percent significance level for entry into the model. If added, they would contribute little to the correlation coefficient and therefore were not used. The final model for the prediction of corn starch conversion was the following:

$$S_e = 158.71 - 3.02\ (MC_e) - 0.59\ (R_1) \qquad (7)$$

where: S_e = starch conversion (%)

MC_e = extrusion moisture content (%)

R_1 = temperature gradient of forward section (°F/inch)

A stepwise regression analysis procedure for analysis of milo starch is shown in Table XII. The variables used were the same as above, but for ground milo. In step one,

TABLE XII

STEPWISE REGRESSION PROCEDURE FOR DEPENDENT VARIABLE S_e (GROUND MILO)

STEP 1 VARIABLE T_1 ENTERED

SOURCE	DF	SUM OF SQUARES	MEAN SQUARE	F VALUE	PR>F	R-SQR
T_1	1	3387.302	3387.302	72.22	0.0001	0.661
ERROR	37	1735.430	46.903			
TOTAL	38	5122.732				

PARAMETER	ESTIMATE	STD ERROR	TYPE II SS	F VALUE	PR>F
INTERCEPT	-116.274				
T_1	0.657	0.077	3387.302	72.22	0.0001

STEP 2 VARIABLE R_2 ENTERED

SOURCE	DF	SUM OF SQUARES	MEAN SQUARE	F VALUE	PR>F	R-SQR
T_1,R_2	2	4022.075	2011.037	65.78	0.0001	0.785
ERROR	36	1100.658	30.574			
TOTAL	38	5122.733				

PARAMETER	ESTIMATE	STD ERROR	TYPE II SS	F VALUE	PR>F
INTERCEPT	-89.114				
T_1	0.518	0.069	1705.410	55.78	0.0001
R_2	1.180	0.259	634.772	20.76	0.0001

STEP 3 VARIABLE T_3 ENTERED

SOURCE	DF	SUM OF SQUARES	MEAN SQUARE	F VALUE	PR>F	R-SQR
T_1,T_3,R_2	3	4466.492	1488.830	79.41	0.0001	0.872
ERROR	35	656.241	18.750			
TOTAL	38	5122.733				

PARAMETER	ESTIMATE	STD ERROR	TYPE II SS	F VALUE	PR>F
INTERCEPT	-28.102				
T_1	0.359	0.063	602.347	32.13	0.0001
T_3	-0.166	0.034	444.417	23.70	0.0001
R_2	1.687	0.228	1026.692	54.76	0.0001

TABLE XII (continued)

STEP 4 VARIABLE T_f ENTERED

SOURCE	DF	SUM OF SQUARES	MEAN SQUARE	F VALUE	PR>F	R-SQR
T_1, T_3, R_2 and T_f	4	4751.480	1187.870	108.79	0.0001	0.927
ERROR	34	371.252	10.920			
TOTAL	38	5122.732				

PARAMETER	ESTIMATE	STD ERROR	TYPE II SS	F VALUE	PR>F
INTERCEPT	89.086				
T_1	0.717	0.085	775.482	71.02	0.0001
T_3	-0.495	0.069	554.133	50.75	0.0001
R_2	-4.855	1.292	154.115	14.11	0.0006
T_f	-182.295	35.683	284.989	26.10	0.0001

T_1 is added to the model first, indicating that discharge temperature was the most highly correlated variable on milo starch conversion. This differed from that found with ground corn, where extrusion moisture was the most highly correlated. This showed that an increased shear due to less moisture did not effect milo starch gelatinization as it did corn starch. The temperature gradient for the rear section of the extruder was determined to be the next most highly correlated variable. It was followed by entrance section temperature and the fractional temperature change in the front end of the extruder barrel. These variables increased the explained variation in the data to 92.75 percent. The F-statistic in this model met a significance level of 99 percent. No other variables met the 85% significance level for entry into the model. The final model for prediction of milo starch conversion was the following:

$$S_e = 89.09 + 0.72\ (T_1) - 0.49\ (T_3) - 4.85\ (R_2) - 182.29\ (T_f) \qquad (8)$$

where: S_e = starch conversion (%)

T_1 = exit temperature (°F)

T_3 = entrance section temperature (°F)

T_f = fractional temperature change in front end (°F)

In the above analyses, product flow rate did not prove to be significant for conversion of corn or milo starch. In the milo starch analysis, all variables that highly correlate with starch conversion included temperature. This showed that milo starch was more easily gelatinized than corn starch. Corn starch conversion was highly correlated with temperature and moisture content, indicating higher shear was necessary for the gelatinization of corn starch.

The optimum extrusion moisture content and extrusion temperature for ground corn and milo were determined by extruding the product at the lowest moisture content possible. The flow must be uniform from the extruder and must not burn. The conditions to achieve this state for ground corn were met at 375°F and an extrusion moisture content of 18 percent. The conditions for ground milo were 310°F at an extrusion moisture content of 18 percent.

Ethanol yields from different extruded samples and non-extruded samples were analyzed with the sole purpose of finding if the extrusion cooking of corn produced any undesirable reaction components at sufficient concentration to adversely affect ethanol fermentation.

The maximum theoretical yield of ethanol from glucose can be calculated from the mass balance which considers all the glucose being converted to ethanol and carbon dioxide.

$$C_6H_{10}O_6 \text{ -----> } 2C_5H_5OH + 2CO_5$$

The mass balance shows that one mole of glucose (180 grams) yields two moles of ethanol (2 X 46 = 92 grams) and two moles of carbon dioxide. The maximum theoretical yield of ethanol from glucose is therefore 0.511 grams EtOH per gram glucose. Actual yield is not equal to maximum theoretical yield because yeasts not only use glucose to produce ethanol but use it to produce other compounds such as glycerol (requiring about 3 percent of the available sugar), amyl alcohol, iso-butanol and traces of other alcohols (Yang, 1981).

Figures 33 and 34 compare proof of the beer after fermentation for extruded corn and milo and non-extruded corn and milo. Each batch cooked test was run under identical conditions. The procedures for atmospheric batch saccharification and fermentation is shown in Appendix A. The procedure for fermentation of extruded grain was similar to Appendix A except the maximum temperature was 150°F and no TAKA-THERM (alpha-amylase) enzyme was used. Alpha-anylase was used mainly for the purpose of controlling viscosity. Viscosity was not a problem with the extruded grain and water slurry, therefore it was not used. As shown in the comparative bar charts, the extruded product for both corn and milo produced a higher proof beer than did the non-extruded (average of 11 percent higher for corn starch and 14 percent higher for milo starch). The proof of beer for corn, on the average, was higher than that of milo (20.6 percent for ground corn as compared to 19 proof for milo). This was due to a higher starch percentage in corn (72.0 percent) than in milo (70.2 percent). Corn also had 1.8 percent natural sugars as compared to 1.4 percent in milo which caused higher proof with corn.

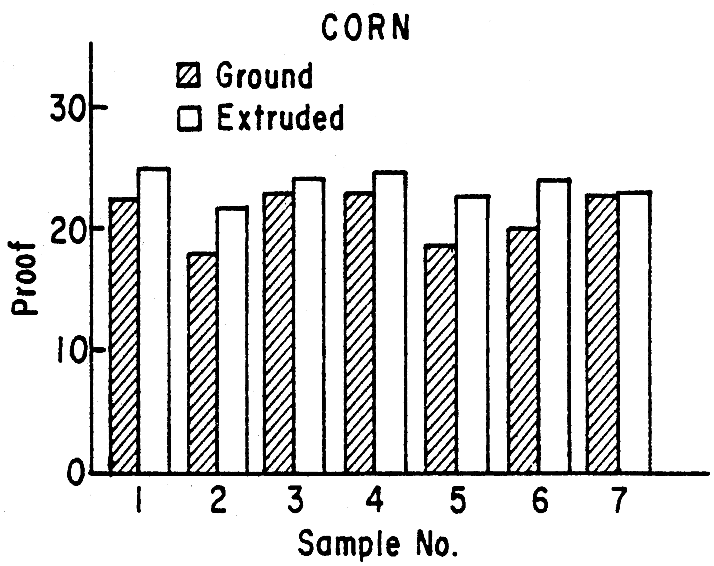

Figure 33. Comparison of fermentation results of extruded corn and non-extruded corn.

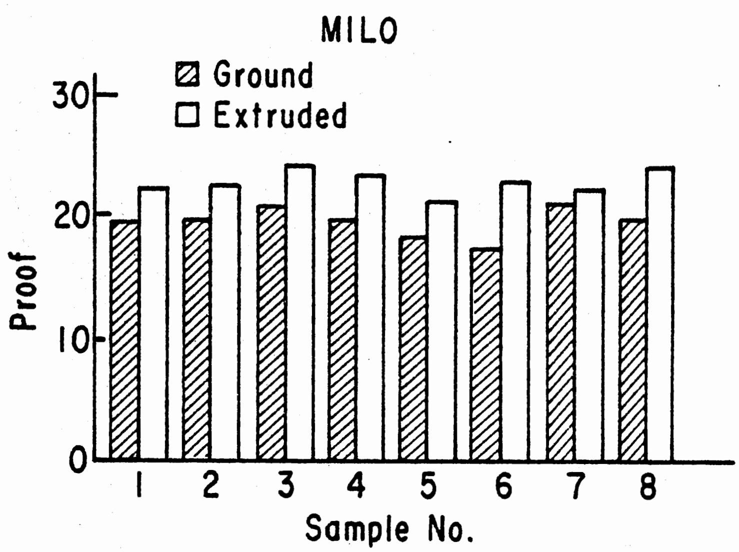

Figure 34. Comparison of fermentation results of extruded milo and non-extruded milo.

CHAPTER VI

CONCLUSIONS

Conversion of corn and milo starch to glucose was determined experimentally at varied moisture contents and steam lock configurations. The effects of moisture contents, temperatures along the barrel, and flow rate were studied. By the use of regression analysis, equations were derived to predict starch conversion.

Yield due to fermentation of extruded milo and corn starch was compared to the yield of a typical atmospheric batch cook system. Also optimum extrusion moisture content and temperature for ground corn and milo were determined.

The following conclusions were reached in the study:

1. The Insta-Pro 500 extruder could be used for cooking ground corn and ground milo which could be converted to glucose by the use of glucoamylase prior to fermentation to ethanol.

2. Corn starch conversion was found to be dependent on extrusion moisture content and temperature gradient in the forward section of the extruder barrel. The mathematical model describing the data was:

$$S_e = 158.71 - 3.02\ (MC_e) - 0.59\ (R_1)$$

where:

S_e = starch conversion (%)

MC_e = extrusion moisture content (%)

R_1 = temperature gradient of forward section (°F/inch)

3. Milo starch conversion was found to be dependent on exit temperature, entrance section temperature, temperature gradient in the rear section of the extruder barrel, and the fractional part of the total temperature change in the front end of the extruder barrel. The mathematical model describing the data was:

$$S_e = 89.09 + 0.72\,(T_1) - 0.49\,(T_3) - 4.85\,(R_2) - 182.29\,(T_f)$$

where

S_e = starch conversion (%)

T_1 = exit temperature (°F)

T_3 = entrance section temperature (°F)

T_f = fractional temperature change in front end (°F)

4. Fermentation of extruded corn yielded and 11 percent increase in beer proof as compared to atmospheric batch cooked samples.

5. Fermentation of extruded milo yielded a 14 percent increase in beer proof as compared to atmospheric batch cooked samples.

6. Optimum extrusion moisture content and temperature for ground corn was 18 percent and 375°F respectfully.

7. Optimum extrusion moisture content and temperature for ground milo was 18 percent and 310°F respectfully.

8. Starch conversion was approximately 8 percent higher for extruded products than for non-extruded products.

9. When using the extruded product in an atmospheric fermentation system, there was no need for alpha-amylase enzymes. These enzymes are used to reduce handling problems associated with highly viscous materials as with non-extruded grain. Viscosity was not a problem when extruded grain was used.

10. The extrusion process, due to the solubility of the extruded grain, suggests that a continuous saccharification process could be implemented, which in turn, suggests a continuous fermentation process.

11. Although wear tests were not conducted, it is suspected that wear of the screw sections, steam locks, and wear rings may be a significant problem for continuous operation with ground corn and milo.

12. Increasing extrusion discharge temperature increased enzyme susceptibility for both ground corn and ground milo.

13. Decreasing extrusion moisture content increased

enzyme susceptibility for both ground corn and ground milo.

14. Decreased the flow rates of grain through the extruder, which increased the residence time, increased enzyme susceptibility for both ground corn and ground milo although flow rate was not found to be a highly correlated variable in the final model selected.

15. Because of the higher yields of the extrusion process compared to the conventional process, extrusion produced ethanol may result in a more cost effective process than conventional produced ethanol.

SELECTED BIBLIOGRAPHY

Banks, W., and C.T. Greenwood. Starch and its Components. Edinburgh, Great Britain: Edinburgh University Press, 1975.

Biocon, Inc., Technical and Product Information P.41.BA. Lexington, Kentucky: Biocon, Inc., 1980.

Chiang, B.Y. and Johnson, J.A. "Measuring Gelatinized Starch by Glucoamylase and O-toluidine Reagent." Cereal Chemistry, 54(3), 429, 1977.

Chiang, B.Y. and Johnson, J.A. "Gelatinization of Starch in Extruded Products." Cereal Chemistry, 54(3), 436, 1977.

Downs, H.W., Clary, B.L. and Whitney, R.W. "Extrusion Cooking for Alcohol Production." presented at the 1980 Summer Meeting of the American Society of Agricultural Engineers, Chicago, Illinois, 1980.

Harper, J.M. Extrusion of Foods. Boca Raton, Florida: CRC Press, Inc., 1981.

Harper, J.M. "Food Extrusion." Critical Reviews of Food Science Nutrition, 11(2), 155, 1979.

Harper, J.M., Rhodes, T.P. and Wanninger, L.A. Jr. "Viscosity Model for Cooked Cereal Doughs." Chemical Engineering Progress Symposium Series, 67(108):40, 1971.

Kerr, Ralph W. ed. Chemistry and Industry of Starch. New York: Academic Press Inc., 1950.

Leach, H.W. "Gelatinization of Starch." Starch: Chemistry and Technology, Volume I, Whistler, R.L. and Paschall, E.F. New York: Academic Press, 1965.

Manners, D.J. "The Biological Synthesis of Starch." Starch and its Derivatives, 4th ed. Ed. J.A. Radley. Great Britain: Chaucer Press, 1968. Pp. 66-90.

McAllister, R.V. "Nutritive Sweetner Made From Starch." Advances in Carbohydrate Chemistry and Biochemistry, Vol. 36. New York: Academic Press, 1979, 15-56.

Mercier, C., and Feillet, P. "Modification of Carbohydrate Components by Extrusion Cooking of Cereal Products." Cereal Chemistry, 52(3), 283, 1975.

Miles Laboratories, Inc. Technical Information on Taka-Therm and Diazyme-100. Elkhart, Indiana: Miles Laboratories, Inc., 1980.

Robyt, J.F., and D. French. "Multiple Attack Hypothesis of Alpha-Amylase Action: Action of Porcine Pancreatic, Human Salivery and Aspergillus Oryzae Alpha-Amylases." Archives of Biochemistry and Biophysics, 122 (1967), 8-16.

Sahagun, J. "Parameters Affecting the Performance of a Low-Cost Extrusion Cooker". M.S. thesis, Department of Agricultural and Chemical Engineering, Colorado State University, Fort Collins, Colorado, 1977.

Tribelhorn, R.E. and Harper, J.M. "Extruder-cooker Equipment," Cereal Chemistry, 25(4):54, 1980.

U.S.D.A., Small-Scale Fuel Alcohol Production, Washington, D.C., 1980.

Whitaker, J.R. Principles of Enzymology for the Food Sciences. New York: Marcel Dekker, Inc., 1972.

Williams, M.A., Horn, R.E. and Rugala, R.P. "Extrusion-an In depth Look at a Versatile Process- Part I," Food Engineering, 49(9):99, 1977.

Williams, M.A., Horn, R.E. and Rugala, R.P. "Extrusion- an In depth Look at a Versatile Process- Part II." Food Engineering, 49(10):87, 1977.

Yang, R.D., Grow, D.A., Goldstein, W.E. "Pilot Plant Studies of Ethanol Production from Whole Ground Corn, Corn Flour and Starch." Presented at the 182nd ACS National Meeting, New York, New York, 1981.

Yellow Springs Instrument Co., Inc. YSI Model 27 Industrial Analyzer Instruction Manual. Yellow Springs, Ohio: Yellow Springs Instrument Co.-Scientific Division, 1975, 1-10.

APPENDIXES

APPENDIX A

GENERALIZED PROCEDURE FOR ATMOSPHERIC BATCH SACCHARIFICATION & FERMENTATION (ADAPTED FROM MILES LABORATORIES TECHNICAL INFORMATION SHEET P820 L-1161)

1. Sterilize all process equipment.

2. Prepare a grain mash by adding (by proportion), 17 gallons of water to 56 lbs. (one bushel) of milled grain (12 to 16 mesh).

3. Adjust this mash to a pH of 6.0 to 6.5 using a 10 percent lime slurry.

4. Add TAKA-THERM at 0.15 percent based on the dry starch content (DSB) of the milled grain.

5. With continuous agitation, begin heating the mash fairly rapidly to 150°F. At this point, decrease the rate of heating to 1.5°F per minute.

6. Continue heating at above rate to a temperature of 205°F and hold for one hour.

7. Add (by proportion), eight gallons of water per bushel of grain.

8. Cool the mash to 140°F and adjust the mash to pH 4.2 with dilute hydrochloric acid.

9. Add 100 ml Diazyme L-100 per 100 lbs. DSB. Hold the mash two hours at 140°F.

10. Cool the grain slurry to 86°F, add yeast in the proportion of 250 grams per 5 bushels, and ferment. Ferment at 86°F - 90°F for 60 hours (or until no carbon dioxide production is observed and the change in solids = 0) with intermittent agitation (3 minutes every 15 minutes).

APPENDIX B

ENZYME RATE TEST PROCEDURE

1. Obtain a sample of extruded grain and dry at 180°F for two hours.

2. Make up two samples of 4 grams of extruded grain in 400 ml. distilled water.

3. Adjust pH with Phosphoric acid to 4.5 - 5.5 (not more than 0.25 ml.).

4. Add 0.5 grams GASOLASE to one, and 1.0 grams GASOLASE to the other. Agitate at room temperature.

5. Starting at time t = 0, measure glucose concentration at 10-minute intervals until readings level off. It will be necessary to make a 1:1 dilution with water just before each reading. Shake gently before reading.

APPENDIX C

STARCH ANALYSIS PROCEDURES FOR DETERMINING THE % STARCH CONTENT IN A SAMPLE OF GRAIN

1. Grind, sieve (0.3 mm pore size) and dry (180°F for two hours) a 50 gr. sample.

2. Solubilize starch with 0.4 Normal NaOH (see Note 1) using 100 ml. per one gram of dry sample, stirring for 1 hour. Use 3 grams of sample.

3. Neutralize with concentrated Phosphoric acid to pH 4.8. Record volume of acid added if greater than 1 ml. for step 7.

4. Add 2.0 grams GASOLASE at near 100°F, and agitate overnight.

5. Dilute a portion of sample 1:1 with water and mix thoroughly.

6. Determine glucose in sample using YSI 27 calibrated at 200 mg./dcl. Readings should be 200 to 500 mg./dcl.

7. Glucose in sample =

(YSI reading) * (TSV / ISV) * 2.0

(see Note 2)
TSV = total sample volume
ISV = initial sample volume

8. % starch in sample =

(mg./dcl. glucose * 0.9) / (% Starch)

(mg./dcl. glucose determined in step 7)

Note 1: 0.4 N. NaOH can be prepared by dissolving 16 grams NaOH in 1 liter of water.

Note 2: For Batch cooked analysis, the initial and the total sample volume will be nearly equal, and no adjustment is necessary. For samples of extruded products and background starch, this adjustment may be important.

APPENDIX D

EXTRUDED SAMPLE ANALYSIS PROCEDURES FOR DETERMINING THE % STARCH CONVERSION IN A SAMPLE OF EXTRUDED GRAIN

1. Grind (small enough to break up any large particles) and dry (180°F for two hours) a 50 gram sample.

2. Add 2 grams of sample to 400 ml. of water at near 100°F. Mix thoroughly and continuously on a magnetic hot-stir plate.

3. Adjust pH to 4.8 with Phosphoric acid, and record volume added if greater than 1 ml for step 5. Add 1/2 gram Gasolase and agitate for 60 minutes (see Note 1) at 100°F.

4. Determine glucose in sample using YSI 27 calibrated at 200 mg/dcl. Readings should be 200 to 500 mg/dcl.

5. Glucose in sample =

(YSI reading) * (TSV / ISV) * 2.0

(see note 2)

TSV = total sample volume

ISV = initial sample volume

6. % starch conversion =

(Glucose in sample * 0.9) / (% Starch)

Note 1: The 60 minute enzyme exposure time assumes no appreciable increase in conversion after 60 minutes. If there is reason to expect that this is not the case, readings should be taken for longer enzyme exposure times and recorded along with the 60 minute reading.

Note 2: For Batch cooked analysis, the initial and the total sample volume will be nearly equal, and no adjustment is necessary. For samples of extruded products and background starch, this adjustment may be important.

APPENDIX E

BATCH COOKED SAMPLE ANALYSIS PROCEDURES

FOR DETERMINING THE % STARCH

CONVERSION IN A BATCH

COOK TEST

1. Obtain about 1/2 pound of ground grain (feedmill grind) and dry at 180°F for two hours.

2. Mix 300 ml water with 90.0 grams grain. Record the empty weight of the sample container, and the weight after added water and grain. Add a small quantity of Calcium Chloride or Calcium Oxide (less than one gram). Add 0.07 ml TAKA-THERM. Adjust pH to 6-7 with NaOH if necessary and record the quantity of NaOH added (if 1 ml or more for determination of total weight of sample in container).

3. Slowly heat to 200°F with vigorous agitation (at about 150-155°F considerable thickening will occur. It may be necessary to heat more slowly during this phase). Hold at 200°F with agitation for 90 minutes.

4. Determine the weight of the sample in the container, and transfer 5% of this amount to another container and mix with a quantity of water equal to (900 - the weight of the mixture transferred + 4.5) in ml. The temperature of the mixture should be near 100°F.

5. Adjust the pH to 4.8 with Phosphoric Acid, and add 1.125 grams Gasolase at near 100°F and agitate for 60 minutes (see Note 1).

6. Determine glucose in sample using YSI 27 calibrated at 200 mg/dcl. Readings should be 200 to 500 mg/dcl.

7. Glucose in sample =

$$(\text{YSI reading}) * (\text{TSV} / \text{ISV}) * 2.0$$

(see Note 2)

TSV = total sample volume

ISV = initial sample volume

8. % starch conversion =

(Glucose in sample * 0.9) / (% Starch)

Notes 1 and 2 are the same as given for extruded samples.

APPENDIX F

ENZYME RATE TEST RESULTS

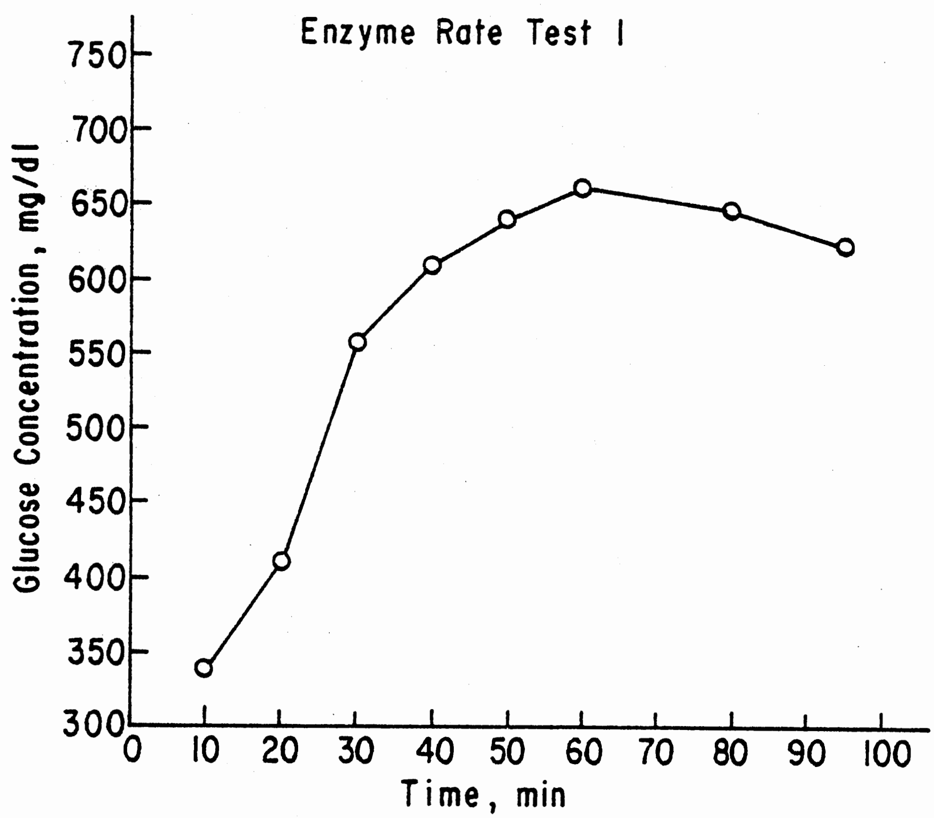

Time	Readings	Average	Total Glucose
10	185	185	339
20	221, 228	225	411
30	300, 309	305	557
40	329, 340	335	612
50	352, 349	351	641
60	355, 368	361	662
80	350, 357	354	647
95	342, 338	340	622

Figure 35. Glucose concentration versus time for extruded corn, 0.5 grams Gasolase, and a dilution of 5 ml. of water to 5 ml. of extruded sample volume.

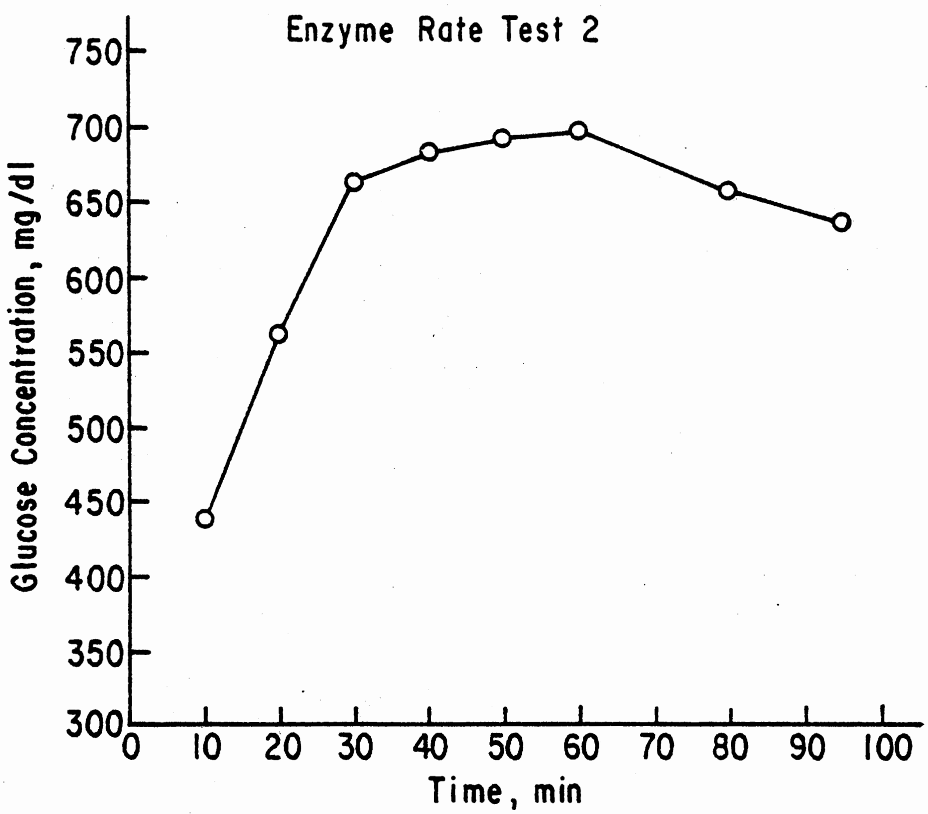

Time	Readings	Average	Total Glucose
10	240	240	439
20	306, 309	308	563
30	364, 365	365	667
40	372	372	681
50	375, 376	376	687
60	382, 377	380	694
80	358, 356	357	653
95	347, 352	350	640

Figure 36. Glucose concentration versus time for extruded corn, 1.0 grams Gasolase, and a dilution of 5 ml. of water to 5 ml. of extruded sample volume.

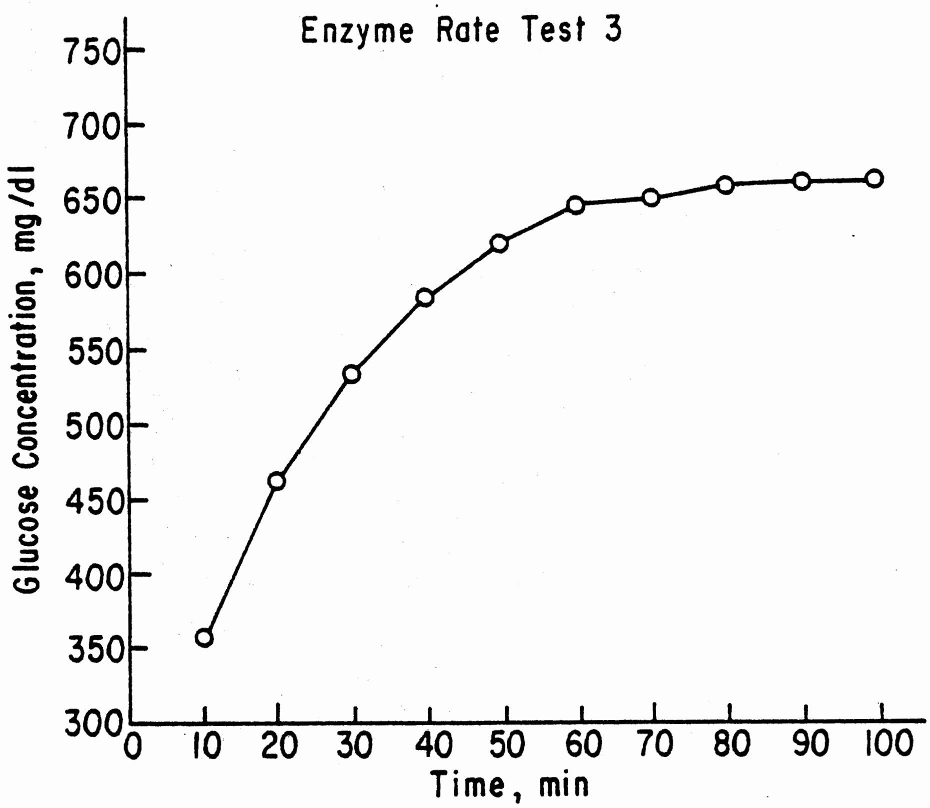

Time	Readings	Average	Total Glucose
10	174, 179, 185	179	358
20	225, 237, 240	234	468
30	263, 268, 274	268	536
40	291, 294, 296	294	588
50	309, 310, 315	311	622
60	320, 323, 328	324	648
70	322, 326, 326	325	650
80	330, 331, 331	331	662
90	332, 333, 335	333	666
100	334, 333, 333	333	666

Figure 37. Glucose concentration versus time for extruded corn, 0.5 grams Gasolase, and a dilution of 10 ml. of water to 10 ml. of extruded sample volume.

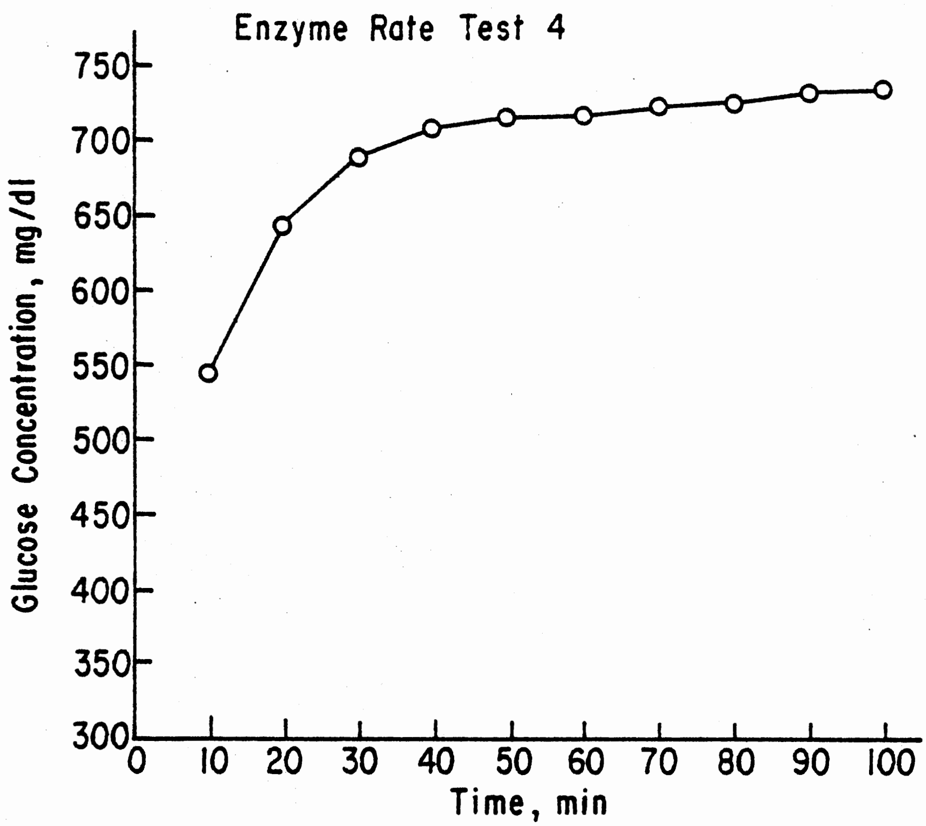

Time	Readings	Average	Total Glucose
10	265, 274, 280	273	546
20	319, 322, 325	322	644
30	344, 346, 344	345	689
40	357, 355, 354	355	711
50	362, 360, 358	360	720
60	355, 361, 359	359	719
70	364, 362, 362	363	725
80	365, 362, 362	363	725
90	365, 366, 367	366	732
100	368, 364, 365	366	732

Figure 38. Glucose concentration versus time for extruded corn, 1.0 grams Gasolase, and a dilution of 10 ml. of water to 10 ml. of extruded sample volume.

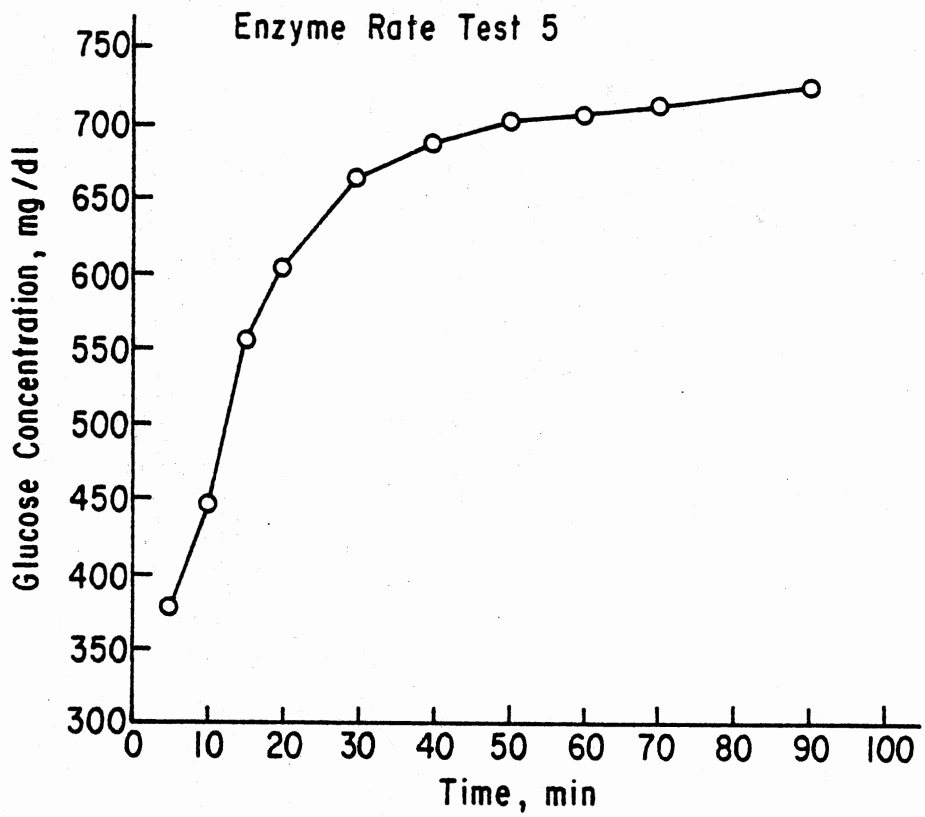

Time	Reading	Total Glucose
5	188	376
10	249	498
15	279	558
20	302	604
30	334	668
40	344	688
50	352	704
60	353	706
70	357	714
90	364	728

Figure 39. Glucose concentration versus time for extruded milo, 0.5 grams Gasolase, and a dilution of 10 ml. of water to 10 ml. of extruded sample volume.

APPENDIX G

MEASURED AND DERIVED RESULTS FROM EXTRUDED GRAIN TESTS, BATCH COOKED TESTS, AND BACKGROUND STARCH TESTS

TABLE XIII

MEASURED AND DERIVED RESULTS FROM EXTRUDED GRAIN TESTS, BATCH COOKED TESTS, AND BACKGROUND STARCH TESTS

N	DA	GT	STE	MC_i	ΔP	$\dot{m}_w$	T_1	T_2	T_3	$\dot{m}_p$	MC_f	G_e	S_e	G_b	S_b	G_i	S_i	MC_e
5	010582	GRCRN	1234	13.9	5	33.75	329.6	226.2	152.2	391.81	10.89	364	89.9	336	82.99	395	72.88	19.84
6	010582	GRCRN	1234	13.9	4	30.5	368	262	146	471.83	9.28	372	91.88	336	82.99	395	72.88	18.44
7	010582	GRCRN	1234	13.9	6	36.75	372	253	145	442.6	10.36	363	89.66	336	82.99	395	72.88	19.64
8	010582	GRCRN	1234	13.9	7	39.5	371.8	249	145	460.14	11.54	357	88.18	336	82.99	395	72.88	19.83
9	010582	GRCRN	1234	13.9	8	42.25	367	243	147	464.15	11.87	367	90.65	336	82.99	395	72.88	20.16
10	010582	GRCRN	1234	13.9	10	47	363	237	151	513.51	10.67	364	89.9	336	82.99	395	72.88	20.19
11	010582	GRCRN	1234	13.9	4	30.5	374	261	145	447.46	9.57	381	94.1	336	82.99	395	72.88	18.67
12	010582	GRCRN	1234	13.9	4	30.5	372.8	247	142	444.71	10.01	365	90.15	336	82.99	395	72.88	18.7
13	010582	GRCRN	1234	13.9	5	33.75	380	249	145	462.36	9.75	369	91.14	336	82.99	395	72.88	18.99
14	010582	GRCRN	1234	13.9	7	39.5	370	240	151	446.84	11.18	355	87.68	336	82.99	395	72.88	19.99
15	010782	GRMLO	1234	14.7	3.25	27.5	290.8	245	125	358.22	8.71	338	83.27	340	83.76	396	73.06	19.94
16	010782	GRMLO	1234.	14.7	3.25	27.5	295.6	241.6	132	360.08	9	355	87.46	340	83.76	396	73.06	19.92
17	010782	GRMLO	1234	14.7	5	33.75	296.8	228.8	133.2	368.82	10.46	326	80.32	340	83.76	396	73.06	20.88

TABLE XIII (continued)

N	DA	GT	STE	MC_i	ΔP	$\dot{m}_w$	T_1	T_2	T_3	$\dot{m}_p$	MC_f	G_e	S_e	G_b	S_b	G_i	S_i	MC_e
18	010782	GRMLO	1234	14.7	4	30.5	299.2	224.4	129.4	357.4	10.2	342	84.26	340	83.76	396	73.06	20.49
19	010782	GRMLO	1234	14.7	3	26.75	306	235.4	138.6	321.48	9.66	363	89.43	340	83.76	396	73.06	20.35
20	010782	GRMLO	1234	14.7	2.25	23.25	310	242.6	141.8	287.76	19.74	371	91.4	340	83.76	396	73.06	20.2
21	010782	GRMLO	1234	14.7	6	36.75	300.8	225.4	135.6	356.43	10.4	358	88.2	340	83.76	396	73.06	21.6
22	010782	GRMLO	1234	14.7	7	39.5	290.4	220.8	129.6	432.73	9.87	336	82.78	340	83.76	396	73.06	20.86
23	010782	GRMLO	1234	14.7	8	42.25	284	226.4	128	437.6	9.6	334	82.29	340	83.76	396	73.06	21.19
24	010782	GRMLO	1234	14.7	10	47	278.8	221.6	145.6	440.15	10.75	311	76.62	340	83.76	396	73.06	21.82
25	010782	GRMLO	1234	14.7	12	51.4	273.2	222.2	151.8	439.33	11.86	311	76.62	340	83.76	396	73.06	22.44
26	010782	GRMLO	1234	14.7	2	21.75	310.6	238.6	135.6	348.53	8.69	355	87.46	340	83.76	396	73.06	19.01
27	010782	GRMLO	1234	14.7	5	33.75	303.8	231.6	137.6	356.67	10.34	318	78.34	340	83.76	396	73.06	21.07
28	010782	GRMLO	1234	14.7	6	36.75	296.6	220.6	132.2	350.37	10.97	291	71.69	340	83.76	396	73.06	21.71
29	010782	GRMLO	1234	14.7	8	42.25	287.2	208.2	142.2	359.15	11.7	298	73.42	340	83.76	396	73.06	22.48
30	012682	GRCRN	1223	14.2	8.75	44	343.2	250.8	224.4	505.56	11.95	338	83.48	340	83.98	395	72.88	20.16
31	012682	GRCRN	1223	14.2	6	36.75	367	236.2	221.6	490.06	8.97	360	88.92	340	83.98	395	72.88	19.39
32	012682	GRCRN	1223	14.2	5	33.75	383.8	240	233	490.27	8.68	367	90.65	340	83.98	395	72.88	18.99

TABLE XIII (continued)

N	DA	GT	STE	MC_i	ΔP	$\dot{m}_w$	T_1	T_2	T_3	$\dot{m}_p$	MC_f	G_e	S_e	G_b	S_b	G_i	S_i	MC_e
33	012682	GRCRN	1223	14.2	8	42.25	381.6	231.8	220.8	555.38	11.38	339	83.73	340	83.98	395	72.88	19.46
34	012682	GRCRN	1223	14.2	9	44.5	384.2	231.6	214	514.8	11.56	344	84.96	340	83.98	395	72.88	20.12
35	012682	GRCRN	1223	14.2	10	47	380.8	227.2	206.4	533.94	12.22	333	82.25	340	83.98	395	72.88	20.23
36	012682	GRCRN	1223	14.2	3	26.75	383.4	258.2	229	492.21	7.35	382	94.35	340	83.98	395	72.88	18.02
37	012682	GRCRN	1223	14.2	4	30.5	375.4	262.4	237.4	514.72	8.25	386	95.34	340	83.98	395	72.88	18.35
38	012682	GRCRN	1223	14.2	12	51.5	375.6	228.4	208.4	543.78	13.68	332	82	340	83.98	395	72.88	20.65
39	012682	GRCRN	1223	14.2	14	56	380.4	215.8	188.8	532.35	14.06	313	77.31	340	83.98	395	72.88	21.3
40	012682	GRCRN	1223	14.2	17	62.25	366.2	201	183	630.22	11.93	302	74.59	340	83.98	395	72.88	20.9
41	042782	GRMLO	1223	10.5	12	51.5	294.2	216.4	154.6	390.01	9.72	292	75.56	346	89.54	377	69.56	19.96
42	042782	GRMLO	1223	10.5	13	53.9	295.6	208.6	157.8	389.25	10.27	244	63.14	346	89.54	377	69.56	20.37
43	042782	GRMLO	1223	10.5	14	56	290.2	200.4	153.4	418.44	10.59	238	61.59	346	89.54	377	69.56	20.07
44	042782	GRMLO	1223	10.5	15	58.1	288.8	195	147.4	419.21	11.11	239	61.85	346	89.54	377	69.56	20.38
45	042782	GRMLO	1223	10.5	16	60.2	284.8	193.2	142	414.97	11.67	232	60.04	346	89.54	377	69.56	20.79
46	042782	GRMLO	1223	10.5	17	62.3	281.2	187.8	141.2	456.99	11.23	232	60.04	346	89.54	377	69.56	20.23
47	042782	GRMLO	1223	10.5	18	64.2	279.2	183.2	139.8	460.25	11.83	231	59.78	346	89.54	377	69.56	20.43

TABLE XIII (continued)

N	DA	GT	STE	MC_i	ΔP	$\dot{m}_w$	T_1	T_2	T_3	$\dot{m}_p$	MC_f	G_e	S_e	G_b	S_b	G_i	S_i	MC_e
48	042782	GRMLO	1223	10.5	19	66.1	277.2	181	138.2	452.72	12.06	230	59.52	346	89.54	377	69.56	20.84
49	042782	GRMLO	1223	10.5	20	68.1	274.6	180.2	135.6	460.79	12.33	230	59.52	346	89.54	377	69.56	20.96
50	042782	GRMLO	1223	10.5	22	72	267.2	176	132.4	454.96	13.44	225	58.23	346	89.54	377	69.56	21.6
51	042782	GRMLO	1223	10.5	24	75.7	264.2	169.4	125.4	444.22	13.71	227	58.74	346	89.54	377	69.56	22.34
52	042782	GRMLO	1223	10.5	26	79.4	262.4	164.2	123.2	448.5	14.08	217	56.16	346	89.54	377	69.56	22.74
53	042782	GRMLO	1223	10.5	28	83	255.6	158.4	116.2	408.62	13.55	200	51.76	346	89.54	377	69.56	22.31
54	042782	GRCRN	1223	10.4	12	51.5	317.8	195	155	409.88	10.35	300	79.75	338	89.85	367	67.71	19.47
55	042782	GRCRN	1223	10.4	13	53.9	325.4	192.2	157.6	422.69	11.05	301	80.02	338	89.85	367	67.71	19.59
56	042782	GRCRN	1223	10.4	14	56	328.6	191.8	158.8	403.3	11.79	320	85.07	338	89.85	367	67.71	20.31
57	042782	GRCRN	1223	10.4	15	58.1	332.4	189.4	152.8	430.16	11.49	312	82.94	338	89.85	367	67.71	20.07
58	042782	GRCRN	1223	10.4	16	60.2	335.6	188.4	150.8	401.42	12.2	304	80.81	338	89.85	367	67.71	21.01
59	042782	GRCRN	1223	10.4	17	62.3	326.4	187.6	144.2	395.84	13.76	306	81.35	338	89.85	367	67.71	21.47
60	042782	GRCRN	1223	10.4	18	64.2	325.6	184.2	140.2	414.14	14.15	304	80.81	338	89.85	367	67.71	21.33
61	042782	GRCRN	1223	10.4	19	66.1	322.4	182	137.4	402.67	13.96	299	79.48	338	89.85	367	67.71	21.89
62	042782	GRCRN	1223	10.4	20	68.1	322.6	179.8	133	412.31	14.53	291	77.36	338	89.85	367	67.71	21.95

TABLE XIII (continued)

N	DA	GT	STE	MC_i	ΔP	$\dot{m}_w$	T_1	T_2	T_3	$\dot{m}_p$	MC_f	G_e	S_e	G_b	S_b	G_i	S_i	MC_e
63	042782	GRCRN	1223	10.4	22	72	322.6	177.8	130.2	415.77	14.45	291	77.36	338	89.85	367	67.71	22.44
64	042782	GRCRN	1223	10.4	24	75.7	321.6	178	126.2	427.14	15.25	291	77.36	338	89.85	367	67.71	22.68
65	042782	GRCRN	1223	10.4	26	79.4	312.2	169.8	116.6	407.43	17.39	275	73.1	338	89.85	367	67.71	23.72
66	042782	GRCRN	1223	10.4	28	83	307.4	164.6	110.2	422.4	17.37	266	70.71	338	89.85	367	67.71	23.81
67	052882	GRMLO	2234	13.9	2	21.7	308	140.2	87.2	395.89	6.01	344	87.63	342	87.12	383	70.66	17.78
68	052882	GRMLO	2234	13.9	3	26.8	307.8	144	86.8	387.76	8.72	348	88.65	342	87.12	383	70.66	18.74
69	052882	GRMLO	2234	13.9	4	30.15	304.6	143.8	86.4	368.44	8.62	325	82.79	342	87.12	383	70.66	19.57
70	052882	GRMLO	2234	13.9	5	33.8	306.6	144	86.2	386.23	9.08	339	86.35	342	87.12	383	70.66	19.93
71	052882	GRMLO	2234	13.9	6	36.8	310.6	144	86	421.94	10.53	322	82.02	342	87.12	383	70.66	19.91
72	052882	GRMLO	2234	13.9	7	39.5	305.4	147	86.2	393.21	11.2	322	82.02	342	87.12	383	70.66	20.75
73	052882	GRMLO	2234	13.9	8	42.2	301.6	145	86.4	406.2	11.85	321	81.77	342	87.12	383	70.66	20.97
74	052882	GRMLO	2234	13.9	9	44.5	300.2	141.6	86.2	401.74	12.13	313	79.73	342	87.12	383	70.66	21.4
75	052882	GRMLO	2234	13.9	10	47	295.8	138.6	86	390.29	13.27	313	79.73	342	87.12	383	70.66	21.99
76	052882	GRMLO	2234	13.9	11	49.2	291.8	135.8	85.8	401.89	13.46	305	77.69	342	87.12	383	70.66	22.11
77	052882	GRMLO	2234	13.9	12	51.6	288.6	134.2	85.8	400.96	13.66	307	78.2	342	87.12	383	70.66	22.49

TABLE XIII (continued)

N	DA	GT	STE	MC_i	ΔP	$\dot{m}_w$	T_1	T_2	T_3	$\dot{m}_p$	MC_f	G_e	S_e	G_b	S_b	G_i	S_i	MC_e
78	052882	GRCRN	2234	13.7	2	21.7	335.8	217	123.6	373.61	8.16	352	88.97	357	90.23	386	71.22	17.82
79	052882	GRCRN	2234	13.7	3	26.8	355.6	230.2	126.2	422.65	8.28	338	85.43	357	90.23	386	71.22	18.18
80	052882	GRCRN	2234	13.7	4	30.5	281.4	125.8	80.2	441.24	9.21	345	87.2	357	90.23	386	71.22	18.56
81	052882	GRCRN	2234	13.7	5	33.8	285.6	132.2	80.6	461	10.45	340	85.93	357	90.23	386	71.22	18.84
82	052882	GRCRN	2234	13.7	6	36.8	284.6	134.6	81.2	467.99	10.96	352	88.97	357	90.23	386	71.22	19.18
83	052882	GRCRN	2234	13.7	7	39.5	282.6	133.6	81.4	464.21	11.07	335	84.67	357	90.23	386	71.22	19.6
84	052882	GRCRN	2234	13.7	8	42.2	280.2	133.8	81.6	457.64	12.33	330	83.41	357	90.23	386	71.22	20.06
85	052882	GRCRN	2234	13.7	9	44.5	274.6	137	82.4	464.92	12.74	343	86.69	357	90.23	386	71.22	20.28
86	052882	GRCRN	2234	13.7	10	47	272.2	138	82.4	457.48	12.96	323	81.64	357	90.23	386	71.22	20.73

2

VITA

John Munger O'Neal

Candidate for the Degree of

Master of Science

Thesis: EFFECTS OF EXTRUSION COOKING OF CORN AND MILO ON ALCOHOL PRODUCTION

Major Field: Agricultural Engineering

Biographical:

Personal Data: Born in Saint Louis, Missouri, March 4, 1956, the son of Dr. and Mrs. R. M. O'Neal.

Education: Graduated from Northwest Classen High School, Oklahoma City, Oklahoma, in May, 1975; received Bachelor of Science in Agricultural Engineering degree from Oklahoma State University in 1980; completed requirements for a Master of Science degree at Oklahoma State University in May, 1983.

Professional Experience: Served as a Graduate Research Assistant and Graduate Teaching Assistant from 1980 to 1983 for the Agricultural Engineering Department of Oklahoma State University. Student Member of Oklahoma Society of Professional Engineers, American Society of Agricultural Engineers and National Society of Professional Engineers. Received an American Society of Agricultural Engineers Blue Ribbon Award in the 1980 Educational Aids Competition. Received the Oklahoma Society of Professional Engineers Outstanding Student Engineering Achievement for 1980.